

Trabajo Fin de Máster

Máster Universitario en Ingeniería Industrial

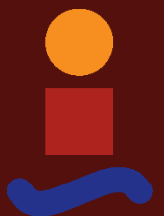
Design and Development of a New ISOLDE Beam Dump

Autor: JM. Martín Ruiz

Tutor: A. Navarro Robles

Dpto. Ingeniería Mecánica
Escuela Técnica Superior de Ingeniería
Universidad de Sevilla

Sevilla, 2024



Trabajo Fin de Máster
Máster Universitario en Ingeniería Industrial

Design and Development of a New ISOLDE Beam Dump

Autor:

JM. Martín Ruiz

Tutor:

A. Navarro Robles

Dpto. Ingeniería Mecánica
Escuela Técnica Superior de Ingeniería
Universidad de Sevilla

Sevilla, 2024

Trabajo Fin de Máster: Design and Development of a New ISOLDE Beam Dump

Autor: JM. Martín Ruiz
Tutor: A. Navarro Robles

El tribunal nombrado para juzgar el trabajo arriba indicado, compuesto por los siguientes profesores:

Presidente:

Vocal/es:

Secretario:

acuerdan otorgarle la calificación de:

El Secretario del Tribunal

Fecha:

Agradecimientos

La elaboración de este documento no habría sido posible sin la ayuda de multitud de personas que me han ayudado directa o indirectamente:

- En primer lugar a toda la sección TCD en el CERN: a Keith y Marco por darme la oportunidad de formar parte de su equipo y aprender tanto, y por supuesto a Ana-Paula por enseñarme a como gestionar un proyecto y mostrarme como enfrentarse a cualquier problema. A todos los compañeros que en algún momento me ayudaron y enseñaron tantas cosas: Nicola, Raffa, Jorge, Claudio, Tobias, Cristina, Ramiro, Tina, Antonio, Rui, Ricardo, Iñigo, Pablo.
- A mi profesor Alfredo por aceptar supervisar este trabajo, por estar siempre disponible para sus alumnos, y por sus siempre buenos consejos.
- A todos mis amigos, dentro y fuera del CERN, que me ayudaron a desconectar y a disfrutar de la vida.
- A toda mi familia por apoyarme, desde cerca o desde lejos, y por supuesto a Rita por hacerme feliz.

Gracias a todos,
Thoiry, 2024

Resumen

La instalación ISOLDE del CERN está equipada actualmente con dos bloques de hierro no refrigerados que actúan como vertederos de haces. Fueron instalados en 1991 y actualmente operan fuera de los parámetros para los que fueron originalmente diseñados. Para garantizar la fiabilidad y la seguridad de la instalación durante los próximos años, se ha realizado un estudio para evaluar el comportamiento de los dispositivos actuales, así como la posibilidad de intercambiar los vertederos de haces de ISOLDE por nuevos modelos durante la Parada Prolongada 3 del CERN. La consolidación también permitiría la compatibilidad con el aumento de energía asociado al PS Booster 2.0 GeV y la actualización de intensidad que se está debatiendo actualmente.

Para evaluar el comportamiento de los dispositivos actuales, se ha realizado un modelo de elementos finitos de los vertederos de haces. Los resultados del estudio de elementos finitos se han comparado con las mediciones de sensores de temperatura colocados en los vertederos de haces, y se han ajustado los parámetros del modelo de elementos finitos para que reflejen mejor el comportamiento medido. Adicionalmente se ha utilizado el modelo de elementos finitos para simular el comportamiento de los vertederos de haces con energías e intensidades más altas, lo cual ha permitido establecer límites racionales para la operación de ISOLDE desde el punto de vista de los vertederos de haces.

Asimismo se propone un nuevo modelo de vertedero de haces que sería compatible con la operación de ISOLDE durante el futuro a medio plazo de la instalación. La propuesta es compatible con todas las restricciones necesarias y se ha hecho un modelo de elementos finitos para evaluar que su comportamiento termo-mecánico sea el adecuado.

Abstract

The CERN ISOLDE facility is currently equipped with two uncooled iron blocks acting as beam dumps. They were installed in 1991 and they are currently operating outside of the original design parameters. In order to guarantee the reliability and safety of the installation for the years to come, a study has been launched to evaluate the behaviour of the current dumps, as well as the possibility to exchange the ISOLDE beam dumps during CERN's Long Shutdown 3. The consolidation would also allow compatibility with the PS Booster 2.0 GeV and intensity upgrade that is under discussion.

To evaluate the performance of the current devices, a finite element model of the beam dump has been carried out. The results of the finite element study have been compared with the measurements of temperature sensors placed in the beam dump faces, and the parameters of the finite element model have been adjusted to better reflect the measured behaviour. Additionally, the finite element model has been used to simulate the behaviour of the beam dumps at higher energies and intensities, which has allowed setting rational limits for the operation of ISOLDE from the point of view of the beam dumps.

A new beam dump model is also proposed that would be compatible with the operation of ISOLDE for the medium-term future of the facility. The proposal is compatible with all the necessary constraints and a finite element model has been made to assess that its thermo-mechanical behaviour is adequate.

Contents

<i>Resumen</i>	III
<i>Abstract</i>	V
1 Introduction	1
1.1 Introduction to CERN	1
1.1.1 Objective	1
1.1.2 CERN organization	1
1.1.3 The CERN accelerator complex	2
1.1.4 The ISOLDE facility	4
2 Simulation approach	7
2.1 Inputs to the finite-element simulations	7
2.2 Beam parameters and energy importation	7
2.3 Steady-state vs transient simulations	9
2.4 Other criteria	10
3 Evaluation of the current ISOLDE dumps	11
3.1 Description of the current ISOLDE dumps	11
3.2 Beam parameters and past studies	14
3.3 Thermocouple installation and tests	15
3.3.1 Thermocouple tests	15
3.4 Thermo-mechanical evaluation and comparison with thermocouple data	18
3.4.1 Geometry, material, and boundary conditions	18
3.4.2 Comparison with tests and parameter adjustment	21
3.4.3 Alternative approach	21
3.5 Model extrapolation to higher energies and intensities	23
3.6 Material limits	23
3.7 Result discussion and conclusions	23
4 Design and thermo-mechanical evaluation of the future dumps	25
4.1 Design constraints	25
4.1.1 Beam parameters	25
4.2 Design concept	26
4.2.1 Early designs	26
4.2.2 Hot Isostatic Pressing	28
4.2.3 Water-cooling vs gas-cooling	28

4.2.4	Simulation with shorter dump	30
4.2.5	Final conceptual design	30
4.3	Finite element modelling	31
4.4	Results	33
4.5	Manufacturing notes	35
4.6	Additional studies	35
4.6.1	Power deposition on the shielding	35
4.6.2	Simulation with target installed	36
4.6.3	Results for five consecutive beam shots	36
5	Conclusions	39
Appendix A	APDL input file	41
A.1	APDL code	41
	<i>List of Figures</i>	59
	<i>List of Tables</i>	61
	<i>Bibliography</i>	63

1 Introduction

The objective of this chapter is to make an introduction of the context in which this work was carried out: first a general introduction of CERN is presented, and then the particular facility and team in which the author worked.

1.1 Introduction to CERN

CERN, Conseil Européen pour la Recherche Nucléaire, is the European Council for Nuclear Research, established in December 1951 at an intergovernmental meeting of UNESCO in Paris. It was born from the idea of creating a world-class physics research facility in Europe, to provide a force for unity in post-war Europe [1]. The CERN convention was initially signed in 1953 by the twelve founding states and since then the total member states number has been growing. Today, there are 23 member states: Belgium, Denmark, France, Germany, Greece, Italy, the Netherlands, Norway, Sweden, Switzerland, the United Kingdom, Austria, Spain, Portugal, Finland, Poland, Slovak Republic, Czech Republic, Hungary, Bulgaria, Israel, Romania and Serbia. The membership involves some duties and privileges. Each member state makes a yearly contribution to the capital and operating costs of CERN's Projects, proportional to their net income. Each of them is represented by two representatives in the Council, which is the decision-making authority. Moreover, there are other associated members such as Cyprus, Slovenia, India, Lithuania, Pakistan, Turkey and Ukraine [2].

1.1.1 Objective

Today, CERN's main area of research is particle physics in an attempt to uncover what the universe is made of and how it works. When it was founded, the structure of matter was not fully known. Since the 60s, CERN research has brought confirmation of different theories: the evidence for the weak force and the electromagnetic force, the discovery of the W and Z particles and the Higgs boson, the particle linked to the mechanism that gives mass to elementary particles, between others. The expertise in particle physics has fostered progress in many other fields. Besides, CERN provides a unique range of particle accelerator facilities to researchers to make science progress. The base of the experiments carried out at CERN is the collision of particles. They can be either protons or ions (although neutrons are also used in certain experiments), colliding between them or against fixed targets. The objective is to increase the number of interactions between particles in order to discover new fundamental particles and validate physical models.

1.1.2 CERN organization

CERN personnel is divided and organized into departments. Each department is structured into groups, and the groups are divided into sections. The work presented in this document was made in the Systems (SY) department, Sources, Targets and Interactions (STI) group, and Targets,

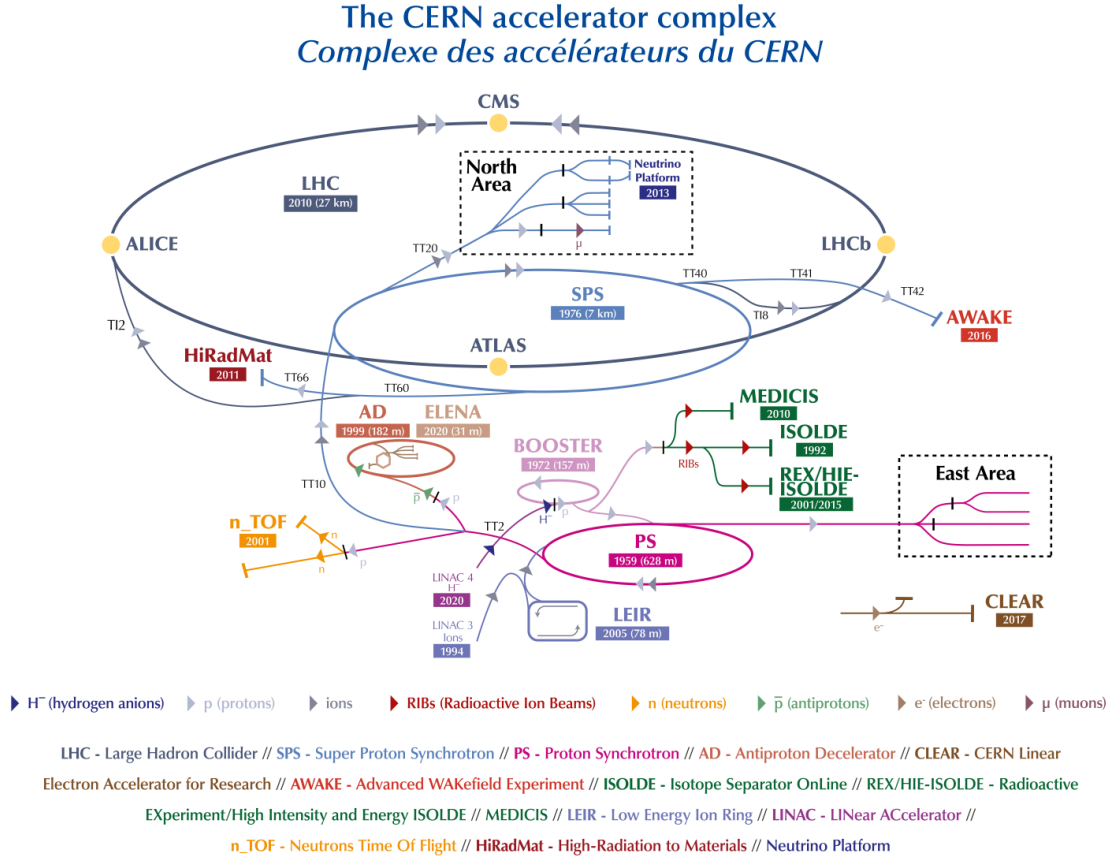


Figure 1.1 The CERN accelerator complex.

Collimators and Dumps (TCD). The TCD section is responsible for all beam-intercepting devices in the CERN accelerator complex, including beam collimators, particle producing targets, beam dumps and absorbers, beam stoppers, passive masks, slits and scrapers. The section carries out conceptual studies, thermo-mechanical studies, manufacturing, installation and maintenance of the mechanical systems and associated equipment, and collaborates in the integration of mechatronics systems needed for operation. The section organizes and undertakes expert interventions in the beam facilities to carry out mechanical repairs or upgrades of its devices. It is also in charge of the conceptual design, R&D activities and operation of fixed target stations as well as of dump/shielding assemblies for the whole CERN accelerator complex. As an integral part of these activities, the section is constantly developing its expertise in the behavior of materials under extreme working conditions as well as their behavior after irradiation (long-term damage and single shot dynamical effects) to predict the evolution of the material response during operation. Research and development activities aiming at the improvement of design of cooling assemblies for beam intercepting devices is also executed in the TCD section.

1.1.3 The CERN accelerator complex

The accelerator complex at CERN is composed by a succession of machines, linear and circular accelerators that propel particles up to 99.9999991% of the speed of light [3]. Particles are injected in the accelerators in bunches. Using powerful magnets, accelerators steer the particles and thanks to the RF cavities, particles are boosted and gradually increase their energy. The particles used are either protons or ions. The CERN complex scheme is shown in figure 1.1.

The Large Hadron Collider (LHC) is the biggest accelerator in the world. It is fed particles that have been previously accelerated in a chain of smaller accelerators. Most of the other accelerators also contain experiments to collide the particles and study their effects. The accelerator chain that feeds the LHC is the following:

- Linac4 is a linear accelerator that accelerates negative hydrogen ions to 160 MeV. Before injection in the next accelerator, the ions are exposed to an electrical field that strips the ions of their electrons to yield protons.
- PSB (Proton Synchrotron Booster) is a circular accelerator that accelerates particles up to 2.0 GeV.
- PS (Proton Synchrotron): circular accelerator that accelerates particles up to 26 GeV/c, with a circumference of 628 m.
- SPS (Super Proton Synchrotron): circular accelerator that accelerates particles up to 450 GeV/c, with a circumference of 6.9 km
- LHC: the largest and most powerful accelerator in the world. It boosts the particles in a loop 27 km in circumference up to an energy of 8 TeV/c.

Protons are not the only particles accelerated in the LHC. Lead ions for the LHC start from a source of vaporised lead and enter Linac3 before being collected and accelerated in the Low Energy Ion Ring (LEIR). They then follow the same route to maximum energy as the protons.

Additionally, there are various other experiments and machines that run in parallel:

- Experiments using particles from the PSB:

- ISOLDE: Online Isotope Mass Separator Facility. This experiment creates a range of isotopes for research and is later described in more detail.
- MEDICIS: facility that contributes to medical research by producing novel radioisotopes, which are used in diagnostics and radiation therapy. It is driven by ISOLDE: a second target is placed downstream of the ISOLDE target, radioisotopes are produced and extracted via mass separation, and then they are implanted in a small foil and delivered to research facilities and local university hospitals.

- Experiments using particles from PS:

- East Area (EA). Composed by several experiments.
- n_TOF is a pulsed neutron source coupled to a 200-metre flight path. It is designed to study neutron-nucleus interactions. The wide energy range and high-intensity neutron beams produced at nTOF are used to make precise measurements of neutron-related processes. Data produced by nTOF are used in astrophysics, in hadron therapy and studies of how to incinerate radioactive nuclear waste.
- DIRAC: to observe and measure lifetime of Muons and Kaons.
- CLOUD: to study possible links between cosmic rays and clouds formation.
- AD is the antimatter decelerator. It receives the particles from PS accelerator and sends them to different experiments:
 - ALPHA: to make, capture and study atoms of antihydrogen and compare them to hydrogen atoms.
 - ASACUSA: to compare anti-protons and protons using antiprotonic helium.
 - ATRAP: to compare hydrogen atoms with their antimatter equivalents.

- Experiments using particles from SPS:

- NA: North Area, where there are a series of primary targets (T2, T4, T6 and T10) which serve different experiments, both for physics and accelerator research.

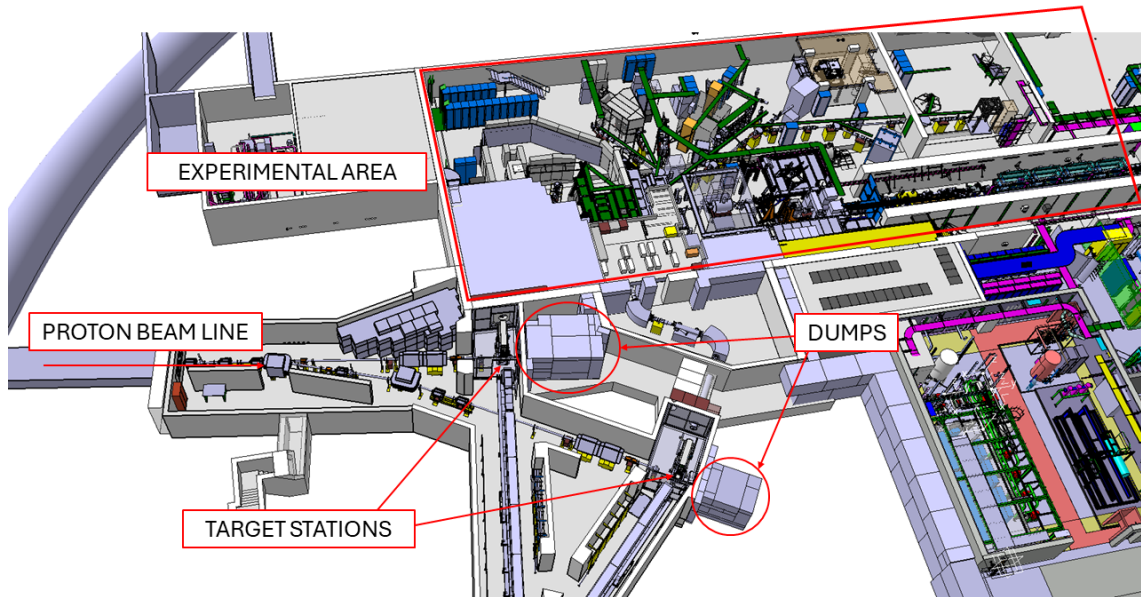


Figure 1.2 General view of the ISOLDE area. The incoming proton beam line and the bifurcation between GPS and HRS lines is visible, as well as the dumps and the experimental area.

- AMBER: experiment to study how elementary quarks and gluons form hadrons (such as protons, pions and kaons) and give these composite particles their distinctive properties.

1.1.4 The ISOLDE facility

The Isotope mass Separator On-Line (ISOLDE) facility produces radioactive ion beams (RIBs) via the isotope separation on-line (ISOL) technique [4]. It allows the study of the vast territory of atomic nuclei, including the most exotic species. Targets made of different materials are bombarded by a pulsed proton-beam with an energy of 1.4 GeV from the PS Booster and an average intensity up to 2 μ A. The facility has two separate target stations. In each of them, different devices are used to ionize, extract, and separate nuclei according to their mass, forming a low-energy beam that is delivered to various experimental stations. The two target stations are named after their mass separator: the general purpose separator (GPS) and the high resolution separator (HRS).

Downstream of the GPS and HRS targets, two dumps are installed in order to safely absorb the remaining beam (up to 62% of the total beam energy if a light target is installed). The ISOLDE facility, like most of the accelerator chain, operates continuously, 24 hours a day and 7 days a week over the whole year. There are some short stops for target exchanges along the year, and there is an annual Year End Technical Stop (YETS). In addition, every few years of operation, there is a Long Shutdown (LS), which is the only opportunity for any significant upgrade to the facility. The ISOLDE target area, and particularly the target stations, are Controlled Radiation Areas, presenting a significant radioactive dose. The dose varies depending on the different conditions and specific location, but in general any inspection or maintenance operation needs to be carefully planned to reduce as much as possible the dose received by any workers.

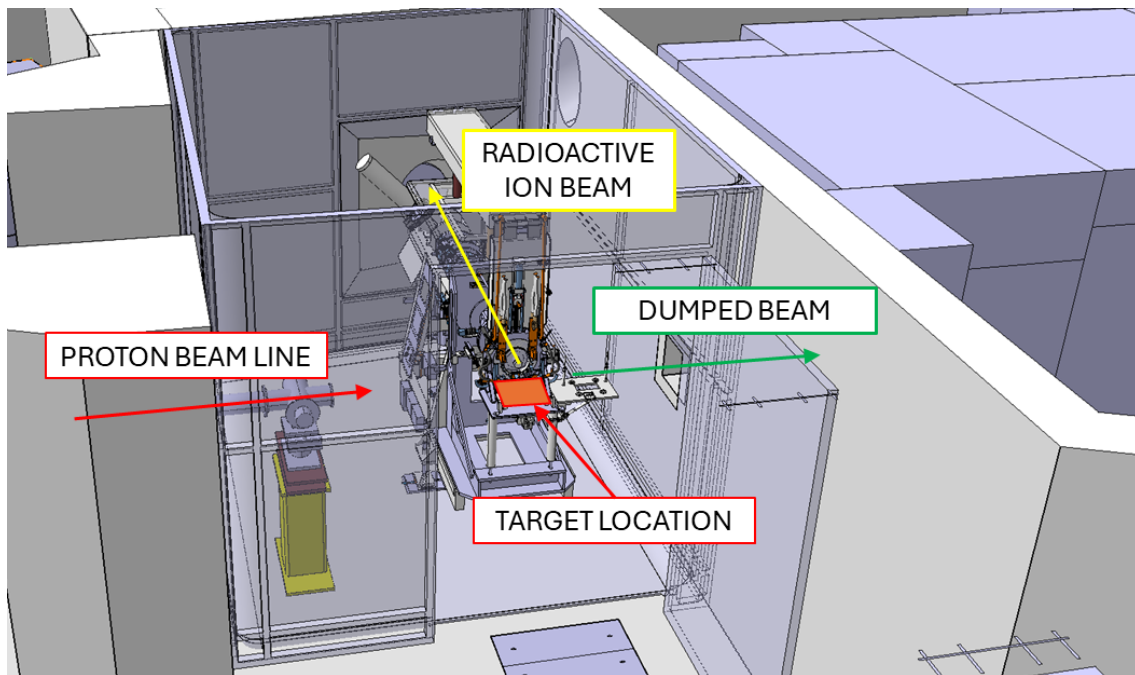


Figure 1.3 View of the GPS target station. The incoming proton beam hits the target, and a percentage of the particles continues straight towards the beam dump. The other fraction of the beam is extracted and steered towards the Experimental Area by a combination of electric and magnetic fields.

2 Simulation approach

The objective of this chapter is to present the common simulation approach that was used for all the thermo-mechanical simulations presented in the following chapters. All the simulations were performed using ANSYS® Mechanical™[5].

2.1 Inputs to the finite-element simulations

The evaluation or design of any Beam Intercepting Device (BID) such as a dump requires a thermo-mechanical simulation. A fundamental input for this simulation is the energy deposited in the material by the impact of the proton beam. The calculation of this energy is performed by a different CERN section, called Beam Machine Interactions (BMI), using the FLUKA Monte Carlo code. Although these simulations were not performed by the author of this work, being such a fundamental input to the thermo-mechanical simulations, a brief introduction will be presented. The FLUKA code is a general purpose Monte Carlo code for the interaction and transport of hadrons, leptons, and photons from keV to cosmic ray energies in any material [6]. The code was first created at CERN in the 1960s and has been developed ever since. It has been built with the aim of including the best physics models in terms of completeness and precision, through a microscopic approach where each step has sound physics bases. Reliability is pursued by comparing with particle production data at single interaction level. FLUKA has a wide range of applications, spanning accelerator design and shielding, radiation protection, particle physics, dosimetry, detector simulation and hadrontherapy.

The output of these simulations is a text file, which divides the full geometry into "bins", in either cartesian or cylindrical coordinates, and states the energy received by each bin in units of energy per volume. An example can be seen in figure 2.1. The size of the bins is adapted as a function of the gradient of the energy deposition, typically having a smaller bin size in the area close to the beam impact. A custom ANSYS plugin (not developed by the author of this work) was used to import this energy and apply it by interpolation to the desired geometry. The custom plugin states the total energy and power applied to the geometry, as well as a graphical representation, which allows the user to check that the energy has been applied correctly.

2.2 Beam parameters and energy importation

For any given simulations, the starting point are the beam parameters. The necessary information for setting up the FLUKA simulation is the following:

- Geometry: in general for the ISOLDE dump simulations, the proton beam would hit either an ISOLDE target and then the dump, or hit the dump directly, depending on which case was being simulated.

```

R-Phi-Z   binning n.   1 "endep.2   ", generalized particle n. 208
R coordinate: from 1.0000E+01 to 2.0000E+01 cm,    10 bins ( 1.0000E+00 cm wide)
P coordinate: from -3.1416E+00 to 3.1416E+00 rad,   36 bins ( 1.7453E-01 rad wide)
Z coordinate: from 0.0000E+00 to 1.5000E+02 cm,   150 bins ( 1.0000E+00 cm wide)
Data follow in a matrix A(ir,ip,iz), format (1(5x,1p,10(1x,e11.4)))

accurate deposition along the tracks requested
1.9709E-06 1.6139E-06 1.2248E-06 8.7969E-07 6.6461E-07 5.3697E-07 3.8637E-07
1.9541E-06 1.5237E-06 1.1805E-06 9.5209E-07 7.0407E-07 5.3760E-07 3.6395E-07
1.8671E-06 1.5607E-06 1.2176E-06 9.0034E-07 6.7699E-07 5.0808E-07 3.8528E-07
(...)

```

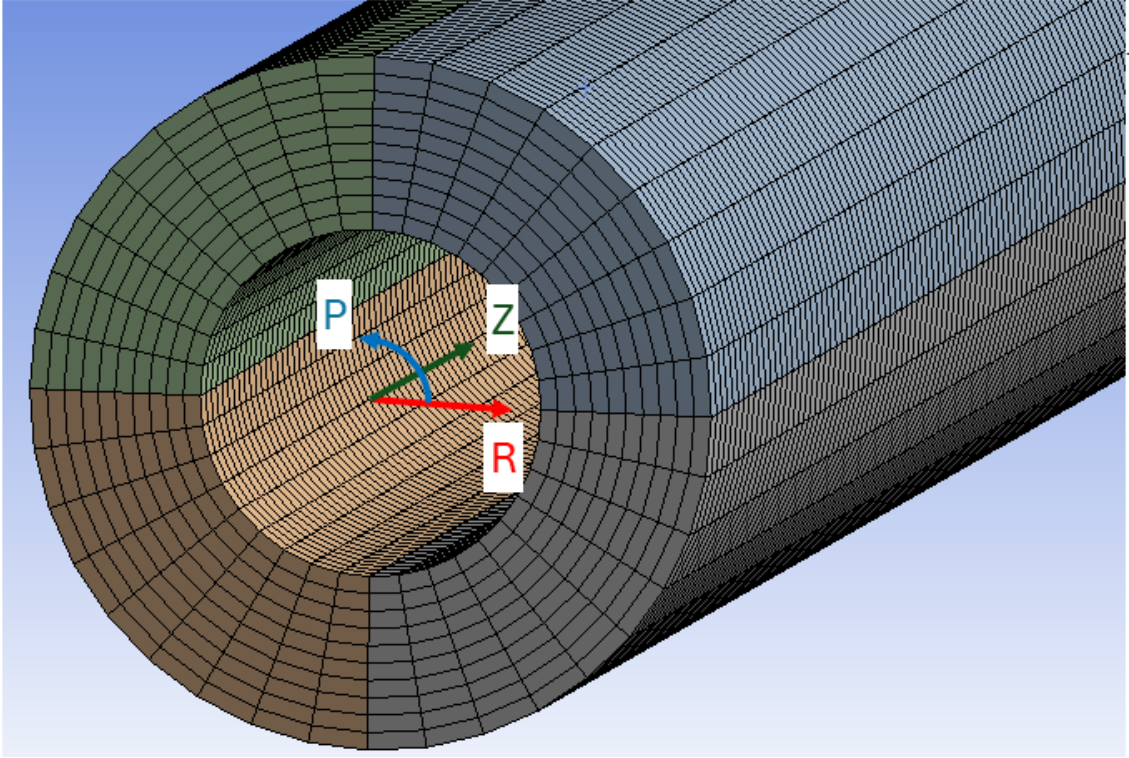


Figure 2.1 On the top, heading and first few lines of the output of a FLUKA simulation. On the bottom, a graphical representation of the cylindrical coordinate system and the resulting geometry division. The inner cylinder is not represented as it was contained in a separate text file with a finer geometry division.

- Beam energy (energy per proton).
- Beam size (typically expressed as a normal distribution).
- Materials (specifically density) that the proton beam or any subsequent particle shower hits.

As previously explained, the output of the FLUKA simulation is a file that for a certain discretization of the geometry gives a value of energy per volume. The FLUKA output is expressed per proton. The actual number of protons and the time structure is later defined in ANSYS. The time structure that has been used for all the simulations can be seen in figure 2.2. It's important to note that this is a simplification, as in reality the distribution of protons inside each bunch is not constant. However, at such short timescales the difference is not significant.

A simple verification was performed systematically to ensure proper energy importation: the total energy imported into ANSYS could be compared to the beam energy, which can be calculated analytically:

$$Energy_{beam}[J] = Energy_{particle}[eV] * Charge_{particle}[C] * n$$

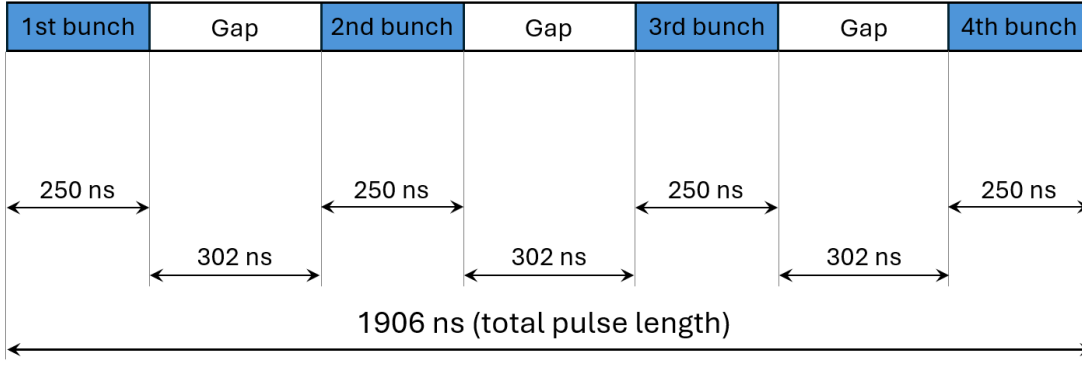


Figure 2.2 Time structure of the pulses which have been simulated. Each pulse consists of four bunches, with gaps in between them. Typically there would be a gap between pulses of either 1.2 or 2.4 seconds.

n being the number of particles. The average power of the beam can be similarly calculated analytically, and it can be useful for cooling calculations:

$$Power_{beam}[W] = Energy_{particle}[eV] * Intensity_{beam}[A]$$

The intensity of a given beam can be easily calculated. For example using the typical parameters for the proposed new dump, the intensity would be:

$$Intensity_{beam}[A] = 1 \times 10^{14} \frac{protons}{pulse} * \frac{1 pulse}{1.2s} * \frac{1.602 \times 10^{-19} C}{1 proton} = 13.3 \times 10^{-6} A$$

And the corresponding beam energy and power would be:

$$Energy_{beam}[J] = 2 \times 10^9 [eV] * 1.602 \times 10^{-19} [C] * 1 \times 10^{14} protons = 32040 J$$

$$Power_{beam}[W] = 2 \times 10^9 [eV] * 13.3 \times 10^{-6} [A] = 26600 W$$

2.3 Steady-state vs transient simulations

The general workflow for thermo-mechanical simulations was to perform a transient thermal simulation, to obtain a time-dependent temperature field across the geometry, which then would be exported to a transient mechanical simulation (see figure 2.3). Depending on the case, either steady-state or transient simulations were used, as illustrated by the following examples:

- **Steady-state simulation:** evaluation of the continuous operation of the ISOLDE dump. The real conditions were one pulse (with a length of approximately 2 μs) every 2.4 s, so the full energy of the pulse was averaged over the 2.4 s. Additional simulations were performed to evaluate how long it took to arrive to the steady-state temperatures.
- **Transient simulation:** evaluation of the conditions right after a beam impact. The full time structure was simulated, including the 4 bunches and the spacing between them. Inside the 250 ns bunch, the energy deposition is averaged to a constant value, which is not completely realistic. However previous calculations and test within the section have proved that this approach is good enough. A small amount of time (approximately 1 ms) was simulated afterwards to leave enough time for the stress to propagate through the material.

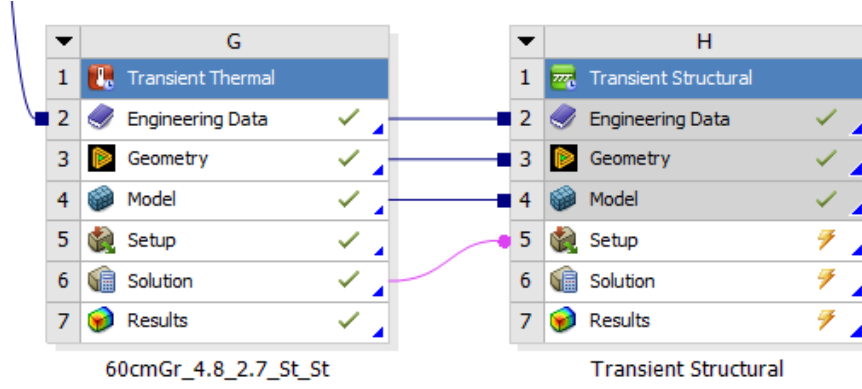


Figure 2.3 Workflow example in ANSYS® Workbench. The results of a transient thermal simulation are imported into a transient structural simulation.

2.4 Other criteria

- Implicit vs explicit simulations. All the simulations presented in this work are implicit. This was chosen due to the relatively long timeframe, in the order of milliseconds.
- Symmetry: symmetry was used whenever possible to reduce the number of elements and hence the computation time.
- Mesh size and time step: the mesh size was chosen carefully, specifically around the beam impact area. In general the elements were linear for the thermal simulations and second-order for the mechanical ones. For the thermal simulations, it was ensured that the following relationship between mesh size (Δx), time step (Δt) and thermal diffusivity was respected:

$$\frac{\Delta x}{\Delta t} \leq \frac{\lambda}{C_p * \rho * \Delta x}$$

C_p being the specific heat capacity, ρ being the material density, and λ being the isotropic thermal conductivity. For mechanical simulations, a similar criteria was used, taking the speed of sound inside the solid as a reference:

$$\frac{\Delta x}{\Delta t} \leq \sqrt{E/\rho}$$

E being the Young's Modulus of the material and ρ being the density.

- Materials: temperature-dependent properties were used whenever necessary. In cases where plastification was possible, a bilinear plastic model was used.
- Failure criteria: the von Mises yield criterion was used for all ductile materials, while the Christensen failure criterion [7] (shown below) was used for the graphite due to its brittleness.

$$\left(\frac{1}{T} - \frac{1}{C}\right)(\sigma_1 + \sigma_2 + \sigma_3) + \frac{1}{2TC}[(\sigma_1 - \sigma_2)^2 + (\sigma_2 - \sigma_3)^2 + (\sigma_3 - \sigma_1)^2] \leq 1$$

T being the uniaxial tensile strength, C being the uniaxial compressive strength, and σ_1 , σ_2 and σ_3 being the principal stress components.

3 Evaluation of the current ISOLDE dumps

This chapter describes the current ISOLDE dumps and provides a thermo-mechanical evaluation of their current operation, including a comparison with measured temperature data.

3.1 Description of the current ISOLDE dumps

There are two dumps in the ISOLDE facility, each of them downstream of the GPS and HRS targets. These two dumps are made by a stack of iron blocks, surrounded by concrete blocks, and buried under 6 m of soil. The dumps were installed in 1991 and there is no active cooling on the blocks.

The existing documentation shows that both dumps are made out of blocks in a range of sizes, as can be seen in figure 3.4. The dump blocks were not manufactured specifically for the purpose, but rather recycled from past CERN projects. The material is quoted as steel, but there is no details on the grade or composition; it is suspected that the blocks might also be made from cast iron, due to the extensive use of that material for shielding blocks at CERN when the dumps were built. The surface roughness of the blocks is unknown. The dump blocks are surrounded by concrete blocks, which are covered with a waterproofing membrane. Only a small fraction of one face of the dumps is accessible, the rest is blocked from view. Up to 2023, there has been no instrumentation monitoring the state of the dumps. In GPS, the target is followed by an irradiation station, while in HRS the main target is followed by the MEDICIS irradiation station [8].

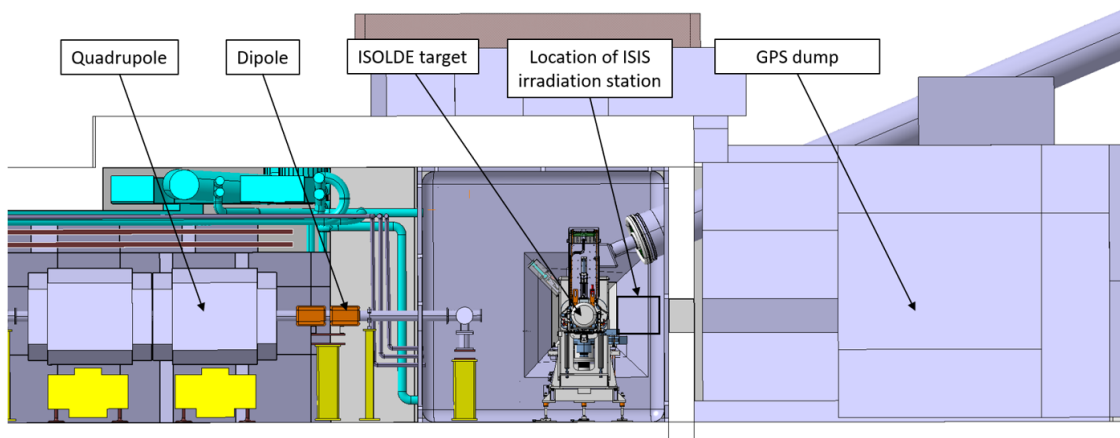


Figure 3.1 Layout of the beam dump downstream of the GPS target position..

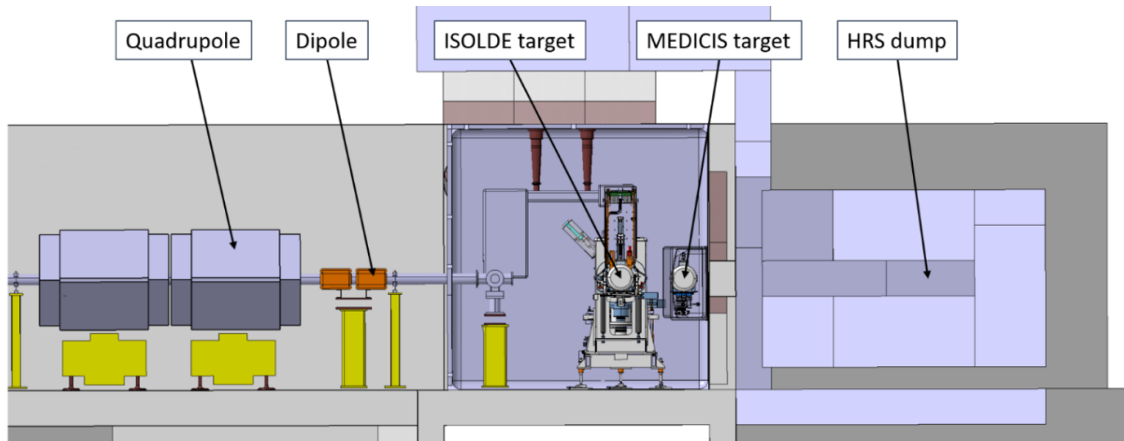


Figure 3.2 Layout of the beam dump downstream of the HRS target position..

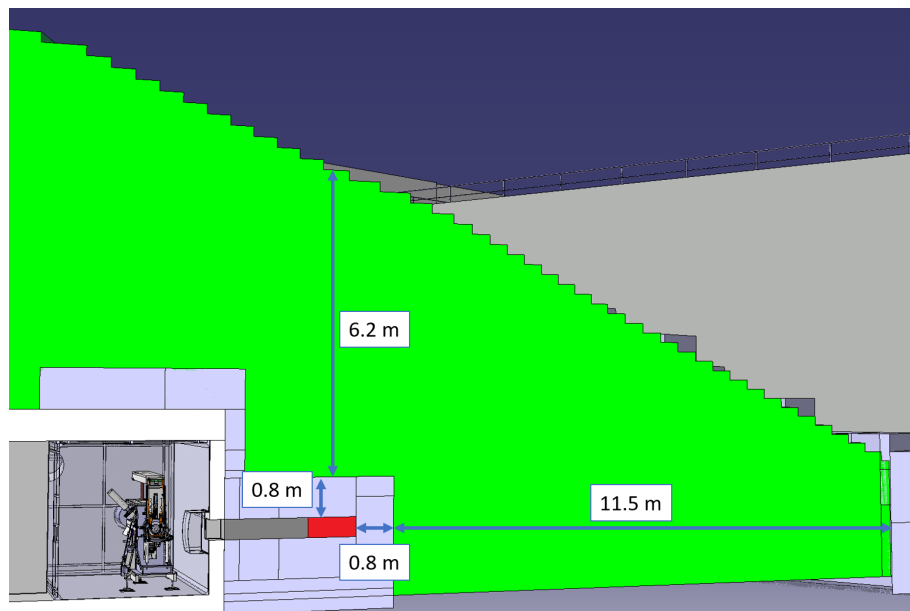


Figure 3.3 Section showing the HRS dump in red, the concrete blocks in grey, and the soil in green..

For both HRS and GPS, there are dipoles towards the end of the beam line which can deflect the beam vertically to hit the ISOLDE target in two locations, see Figure 3.5:

- The target container, which is aligned with the ‘normal’ beam position.
- The neutron converter, which is used for different experiments and is located approximately 21-26 mm below, depending on target construction.

As shown in Figure 3.1 and Figure 3.2, the front face of the steel dump blocks is located approximately 3 m downstream of the target positions totalling a 4 m passage for the beam in air from the vacuum window at the end of the beam line (about 2 m inside the Faraday cage and 2 m within the shielding assembly after the Faraday cage). For GPS, a thin aluminium plate with a thickness of 1 mm obstructs the opening in the Faraday cage, 2 m upstream of the dump blocks. For HRS, a rounded aluminium cover encloses the MEDICIS irradiation station (see Figure 3.6) which is itself separated from the dump enclosure by a 1 mm-thick aluminium plate.

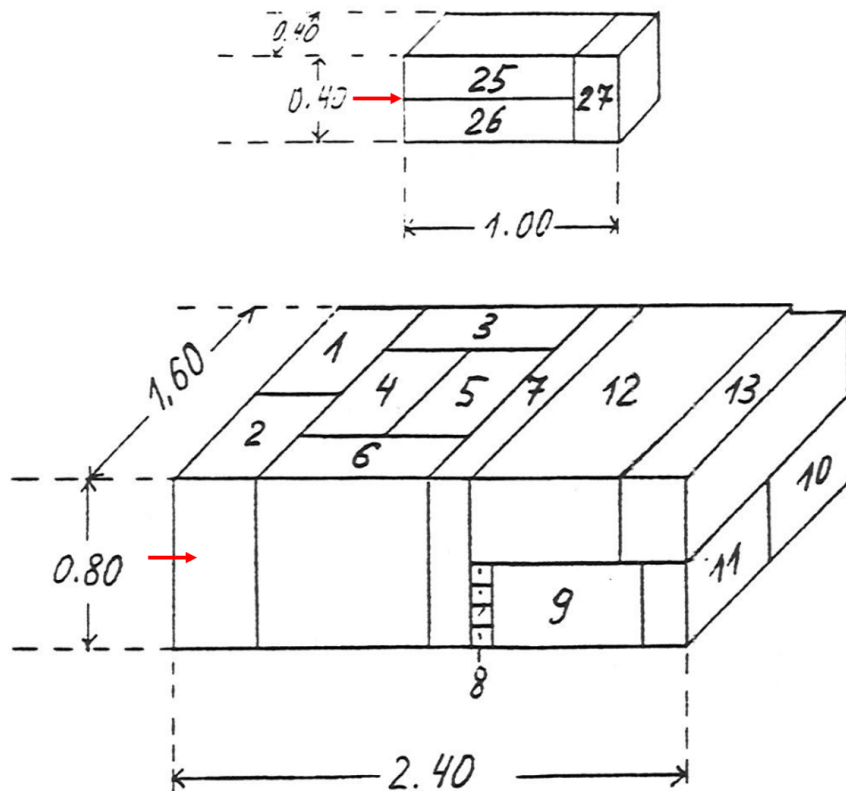


Figure 3.4 On the top, the HRS dump blocks. On the bottom, the GPS dump blocks. The concrete blocks are not shown. The red arrow shows the direction of the beam. The dimensions shown are in meters.

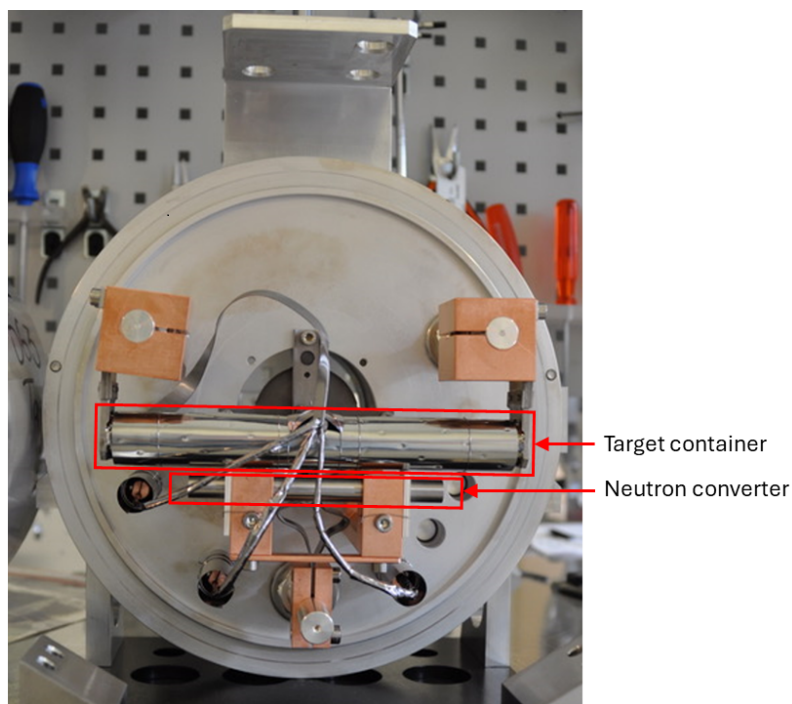


Figure 3.5 ISOLDE target: the upper, longer cylinder is the target container, while the shorter cylinder is the neutron converter.



Figure 3.6 Picture of the HRS Faraday cage with the cover for MEDICIS target irradiations..

3.2 Beam parameters and past studies

When originally installed in 1991, both the shielding and beam dump designs were based on the availability of 3.2×10^{13} protons/pulse at 1 GeV every 2.4 s, corresponding to an intensity of $2.1 \mu\text{A}$ and a beam power of 2.1 kW [9]. As can be seen in table 3.1, the current beam parameters are higher than that; in addition, the accessible dump faces show signs of corrosion and condensation is visible on the area. For these reasons, a re-evaluation of the thermomechanical performance of the dumps has been performed.

Table 3.1 Current and future operating parameters..

Scenario	Beam energy	Beam intensity	Beam power
Current	1.4 GeV	$2 \mu\text{A}$	2.8 kW
Future	2.0 GeV	$6 \mu\text{A}$	12 kW

A study of the thermo-mechanical performance of the dumps was performed in the past [10]. However, that study considered steady-state thermal simulations with no target inserted, which is overly conservative. The time to reach a steady-state varies with different intensities and energies, but is in general between 24-48 hours. During ISOLDE operation, the only time that the facility is operated without a target inserted are short tests at low intensities (SEM grid tests, which generally take less than 4 hours), so the temperatures predicted in that report would never be achieved during operation. In this document, the performance of the dumps will be evaluated at higher energies up to 2.0 GeV and higher intensities up to $13.4 \mu\text{A}$. The worst-case scenario that will be studied is a steady-state with a very light target inserted (target #650 has been identified as the lightest target installed in ISOLDE up to now, its characteristics are reflected in table 3.2). This has been identified



Figure 3.7 Thermocouple (center) with two magnets at each side. The thermocouple itself also includes magnets above and below..

as a realistic scenario, as during physics runs ISOLDE typically operated for one week with the same target installed.

Table 3.2 Data for the target that was used in the simulations in this chapter..

Target	Target material material mass	Target dimensions	Shape and material	Container
ISOLDE Target #650	Multi-walled carbon nanotubes	0.01485 kg	Cylinder $\varnothing 15 \times 168$ mm	Tantalum

3.3 Thermocouple installation and tests

Two type-K thermocouples were installed in the visible face of each of the dumps in March 2023, in order to control the operation of the dump and compare the results with the simulations. The thermocouples are fixed to the dump surface using rad-hard SmCo magnets, as other types of magnets can be damaged by the high radiation dose in the area. The relative position of the thermocouples with respect to the beam position could not be precisely measured due to the difficult access and high radioactive dose in the area. In the first few months of operation, the measured temperatures have been realistic and coherent with the beam operation schedule.

The thermocouples are connected to the NXCALS database, which allows to control the temperature in real-time as well as logging and visualization alongside other variables (for example the beam intensity).

3.3.1 Thermocouple tests

The thermocouples capture and log data 24 hours a day and 7 days a week, hence any type of ISOLDE operation could be used to benchmark the simulations. However, during typical ISOLDE physics run there is a target installed (which introduces more complexity in the Monte Carlo simulations) and the intensity can be very variable as a function of the physics needs. Therefore, two dedicated tests were performed: a 1.4 GeV beam was sent directly to the dumps with no ISOLDE target installed for 12-14 hours, and then allowed to cool back down to room temperature. The objective was to keep a constant beam intensity of $2 \mu\text{A}$ during the whole test, however due to operational issues upstream of the ISOLDE facility, the beam intensity fluctuated slightly, as seen in Figure 3.11



Figure 3.8 GPS dump face with both thermocouples installed..



Figure 3.9 HRS dump face with both thermocouples installed..

and Figure 3.13. The test in GPS happened on 20/03/2023 and lasted 12 hours. The beam size at the SEM grid was recorded at the start of the test ($\sigma_x = 5.4$ mm, $\sigma_y = 3.8$ mm):

The test in HRS happened on 23/03/2023 and lasted 13.5 hours. The beam size at the SEM grid was recorded at the start of the test ($\sigma_x = 2.6$ mm, $\sigma_y = 1.8$ mm).

The temperatures recorded will be presented later in the document and compared with the finite



Figure 3.10 Installation of the thermocouples. The long arm used to insert the thermocouple is visible on the photo..

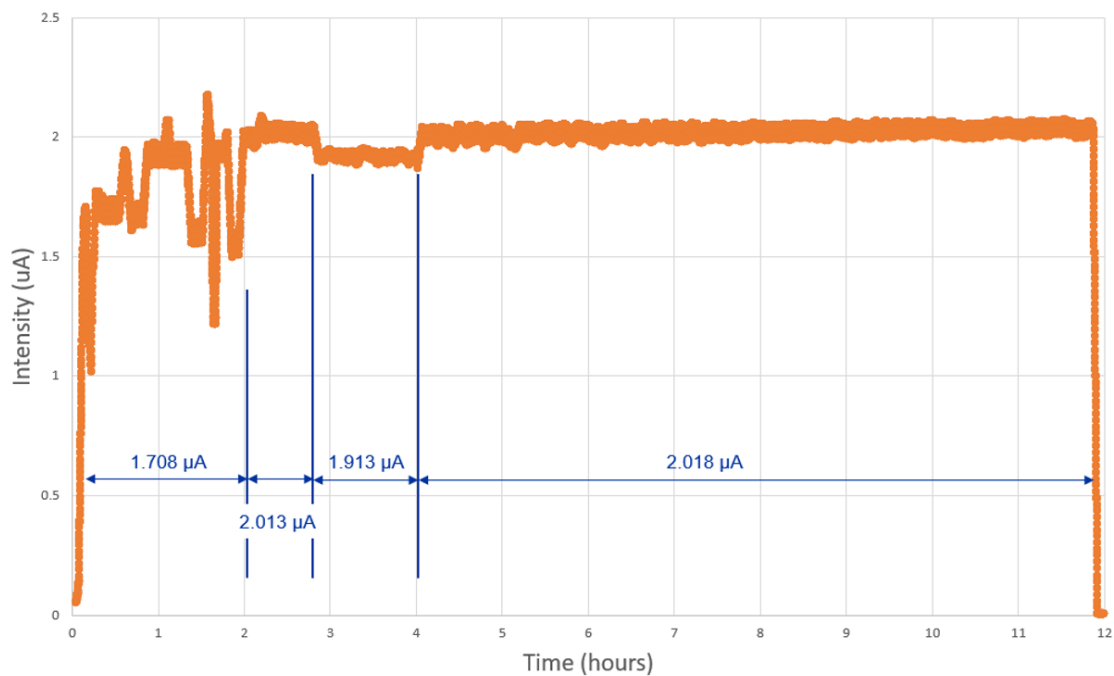


Figure 3.11 Intensity recorded during the GPS test..

element simulations. The thermocouples will continue to capture data in the rest of the 2023 ISOLDE physics run.

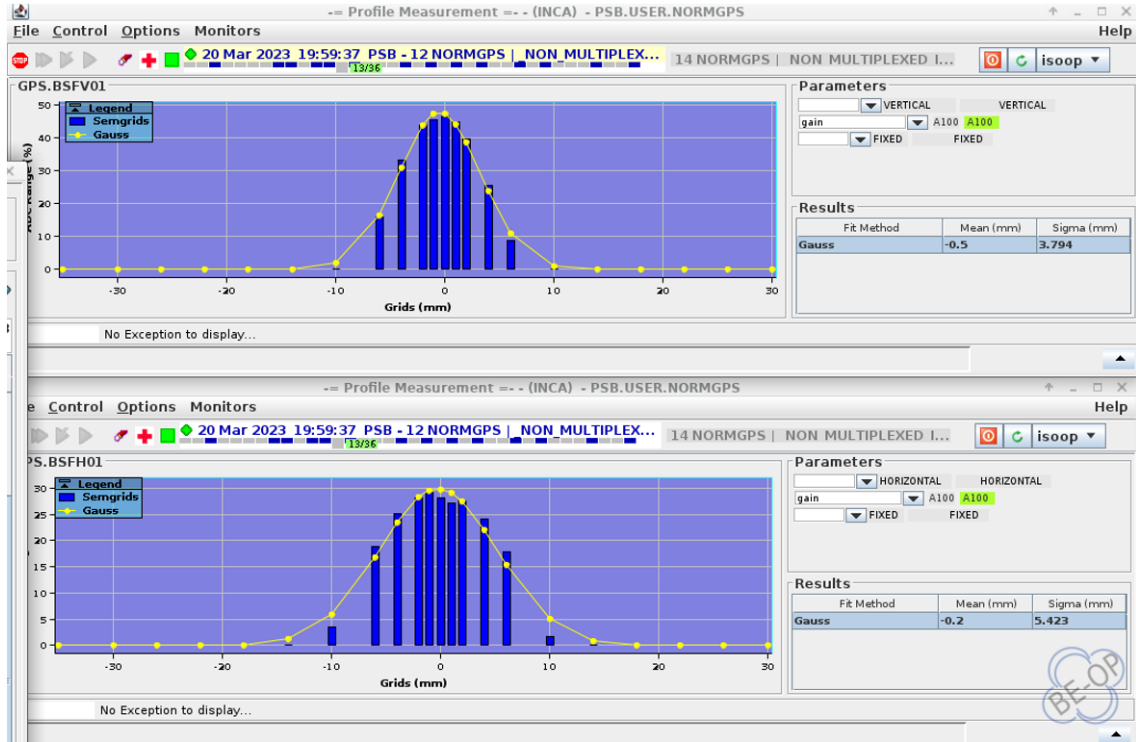


Figure 3.12 Beam size recorded during the GPS test..

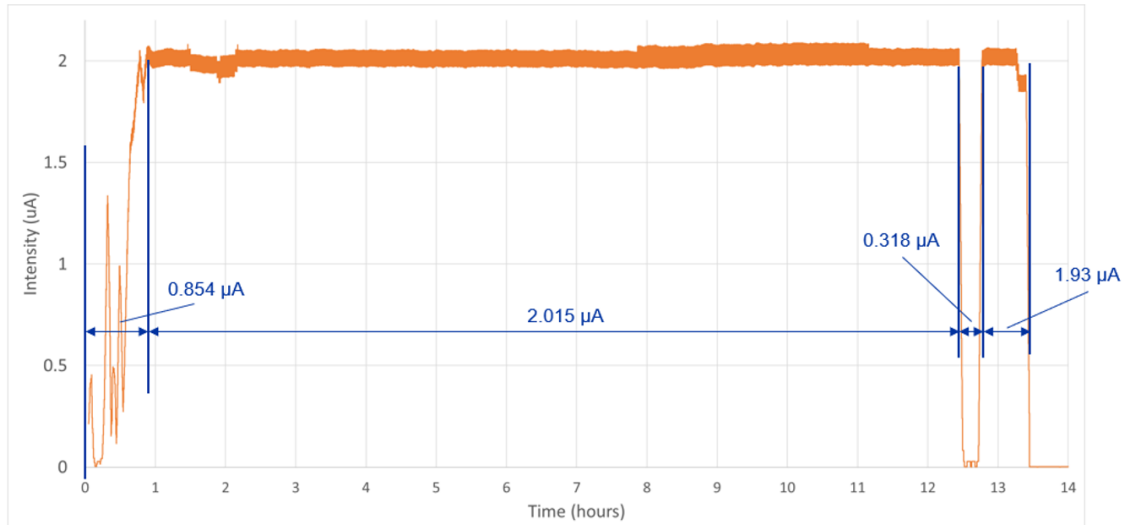


Figure 3.13 Intensity recorded during the HRS test..

3.4 Thermo-mechanical evaluation and comparison with thermocouple data

3.4.1 Geometry, material, and boundary conditions

The dump blocks were not manufactured specifically for the purpose, but rather recycled from past CERN projects. The geometry and sizes are described in the drawings available in [11, 12]. However, some inconsistencies exist between those drawings and the ones found in [13]. The latter is considered to be more reliable, as it's more recent and it better reflects what can be seen in the photos of the area. The block material is quoted as steel. However, shielding blocks used at

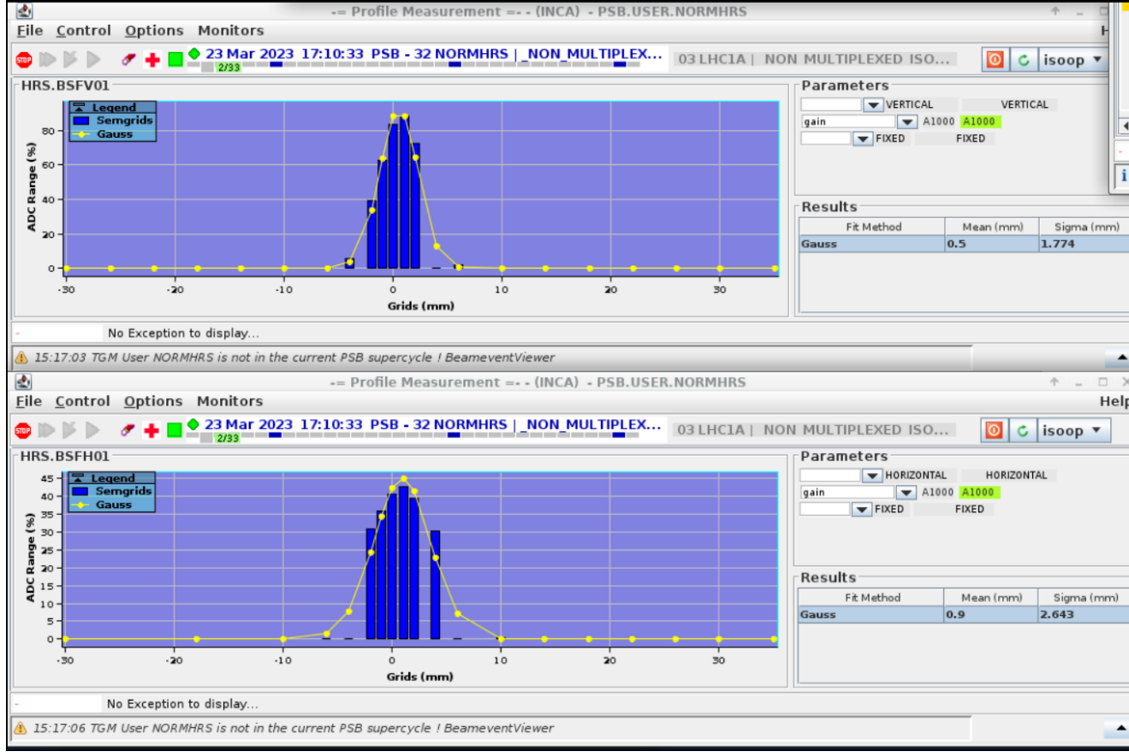


Figure 3.14 Beam size recorded during the HRS test..

CERN are typically made from cast iron, so that material has also been studied as a possibility. The specific grade is not known. The surface roughness of the blocks, which has an effect in the heat transfer between blocks, is unknown. The dump blocks are surrounded by concrete blocks, which are covered with a waterproofing membrane. The assembly is covered by roughly 6 m of soil. The upstream face of the dumps where the beam hits is visible, but the rest of the blocks are not accessible. For both dumps, the entire dump blocks were simulated, along with the concrete blocks below and above.

A fixed temperature boundary condition was setup on the outer boundary. For HRS, it was considered that the earth surrounding the dump was at a fixed temperature of 13 °C, as the soil around the dumps at a 6 m depth will remain at a constant temperature equal to the mean temperature in the area [14, 15]. For GPS, as the dump is surrounded by buildings (Target Area and building 170), it was considered that the fixed temperature was 24 °C.

The thermal contact conductance (TCC) values between the dump blocks, and between the dump and concrete blocks, were calculated based on semi-empirical formulations [16]. These formulations estimate the value of the TCC based on the surface and mechanical properties of the 2 surfaces, the pressure between them, and the gas (in this case air) that fills the small voids in-between. Both the solid spot thermal conductance and the gap conductance at the interface were considered. The solid spot thermal conductance values were based on:

$$h_s = 1.13 \left(\frac{k \tan \theta}{\sigma} \right) \left(\frac{P}{H} \right)^{0.94}$$

for plastic deformation, and:

$$h_s = 1.55 \left(\frac{k \tan \theta}{\sigma} \right) \left(\frac{P \sqrt{2}}{E' \tan \theta} \right)^{0.94}$$

for elastic deformation.

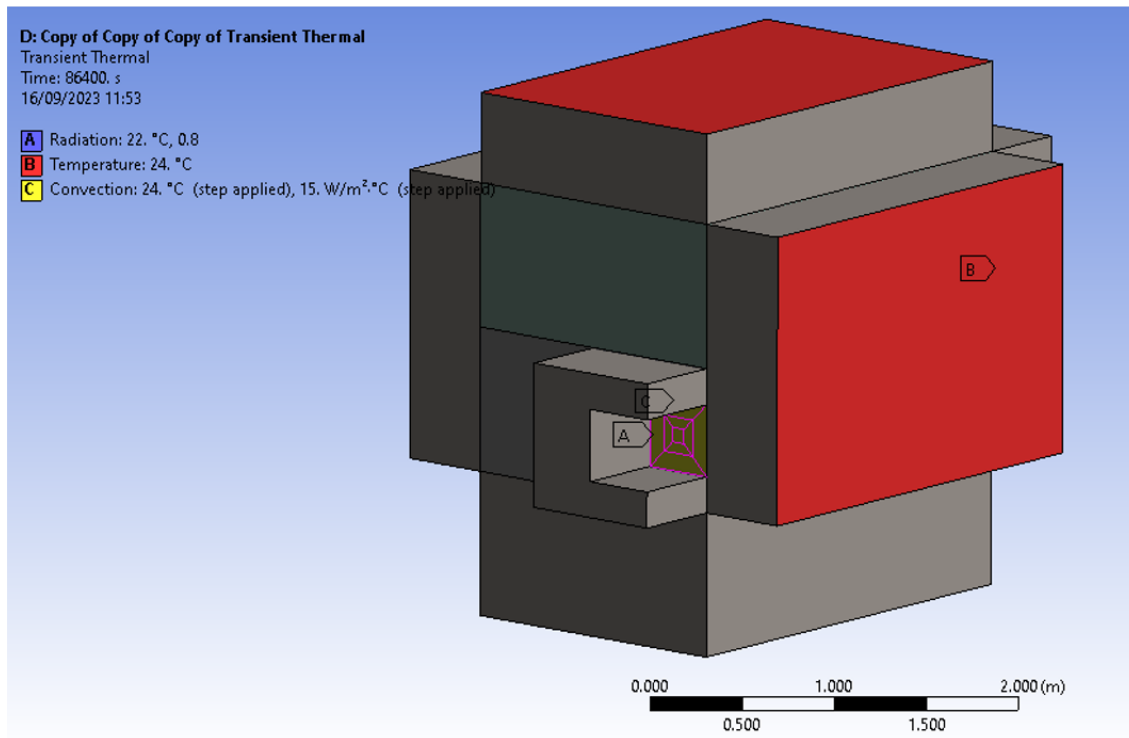


Figure 3.15 GPS setup.

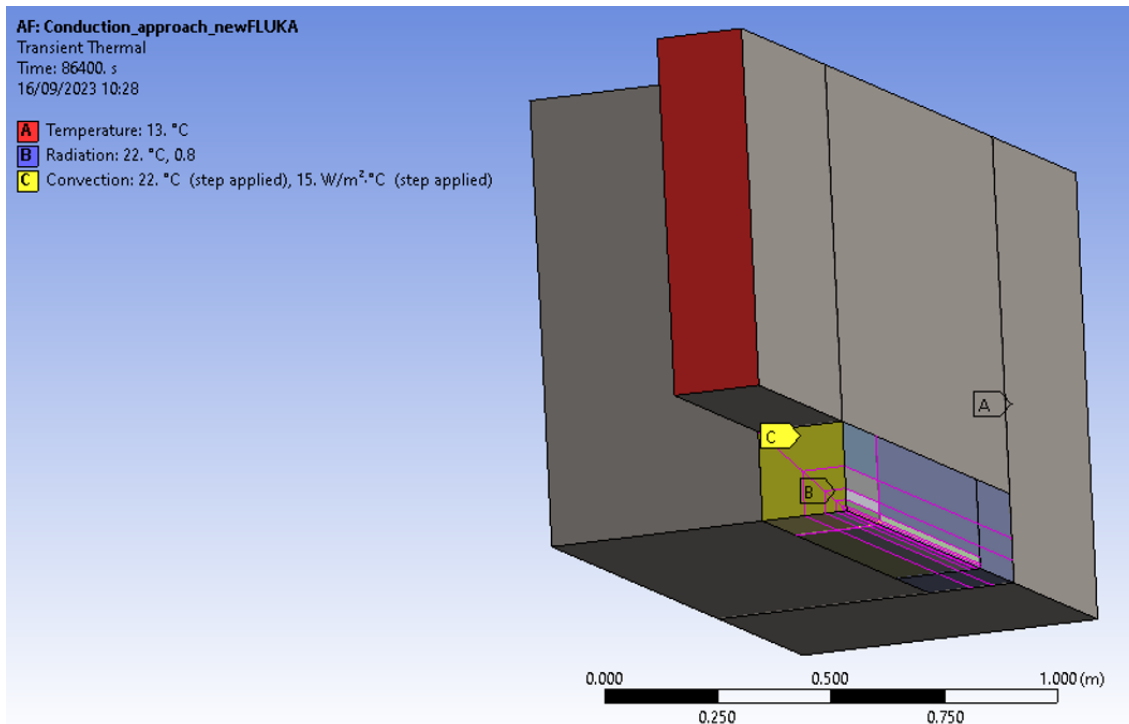


Figure 3.16 HRS setup. 2 planes of symmetry were used..

The gap conductance values were based on:

$$h_g = k_g / (\delta + g_1 + g_2)$$

$$g = \left(\frac{2-\alpha}{\alpha}\right)\left(\frac{2}{\gamma+1}\right)\left(\frac{k_g}{\mu C_v}\right)\lambda$$

The values of k being the harmonic mean thermal conductivity of both materials, σ being the standard deviation of the surface asperity heights, $\tan\theta$ being the mean absolute slope of the profiles, P being the pressure between both materials, H being the microhardness, E' being the reduced modulus of elasticity of both materials, and k_g being the thermal conductivity of the gas (air in this case). Both the values of solid spot and gap conductance were summed to obtain the total thermal contact conductance.

Convection and radiation cooling were applied on the upstream face. The emissivity value for the dump blocks was fixed at 0.8. The material properties were chosen inside realistic ranges for both steel and cast iron.

3.4.2 Comparison with tests and parameter adjustment

In order to compare with the test data, two transient-thermal simulations were performed, using the intensity data from Figure 3.11 and Figure 3.13. To take into account the fluctuations in intensity, each test was broken in 4 stages, and an average intensity was considered for each stage. Two different FLUKA simulations were used as input, with the corresponding GPS and HRS geometries. The dump block material was considered as steel, with a density of 7.8 g/cm^3 . The energy deposition was applied on the dump blocks (not on any of the surrounding concrete). The beam size used for GPS was slightly different to the one used in the test ($\sigma_x = 2.3 \text{ mm}$, $\sigma_y = 5.8 \text{ mm}$ at the dump face, not the SEM grid). However, it's considered that over 12 hours the beam size difference will not be significant. The beam size used for HRS was the same as the one used in the test.

Due to the mentioned uncertainties around the dump block geometry, material properties, and surface roughness, the cooling parameters (external temperature, TTC) and material properties (specific heat and conductivity) were initially estimated and then later corrected with data from the thermocouple measurements.

Table 3.3 Parameters used in both simulations..

Parameter	GPS	HRS
Exterior temperature	24 °C	13 °C
TCC between dump blocks	150 W/m ² · K	1500 W/m ² · K
TCC between dump blocks and concrete	100 W/m ² · K	1000 W/m ² · K
HTC (visible dump face)	15 W/m ² · K	
Convection ambient temperature	24 °C	22 °C
Radiation ambient temperature	22 °C	
Emissivity	0.8	
Concrete conductivity	2.5 W/m · K	2.9 W/m · K
Concrete heat capacity	780 J/kg · K	
Dump block conductivity	Temperature-dependent, 57.2 W/m · K at 100 °C	
Dump block heat capacity	620 J/kg · K	

Using the parameters found in Table 3.3, the simulated temperatures agreed with the measured data within 20%. Figures 3.11 and 3.13 show the comparison between the thermocouple measurements and the expected evolution of the temperature according to the model in both dumps.

3.4.3 Alternative approach

A simpler approach was also tested in which only the dump blocks were simulated, using convection around every outer face. However, it was found that the results did not agree well with the measured

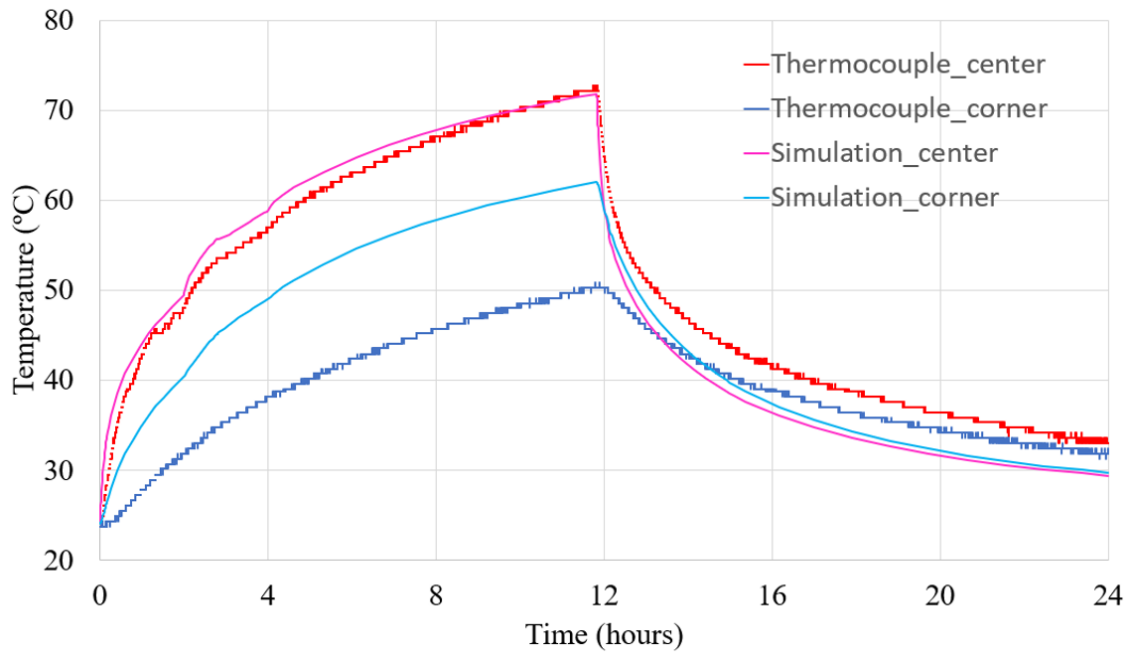


Figure 3.17 Graph showing the temperature evolution measured by the thermocouples vs the temperature simulated by the finite element simulation in the GPS dump..

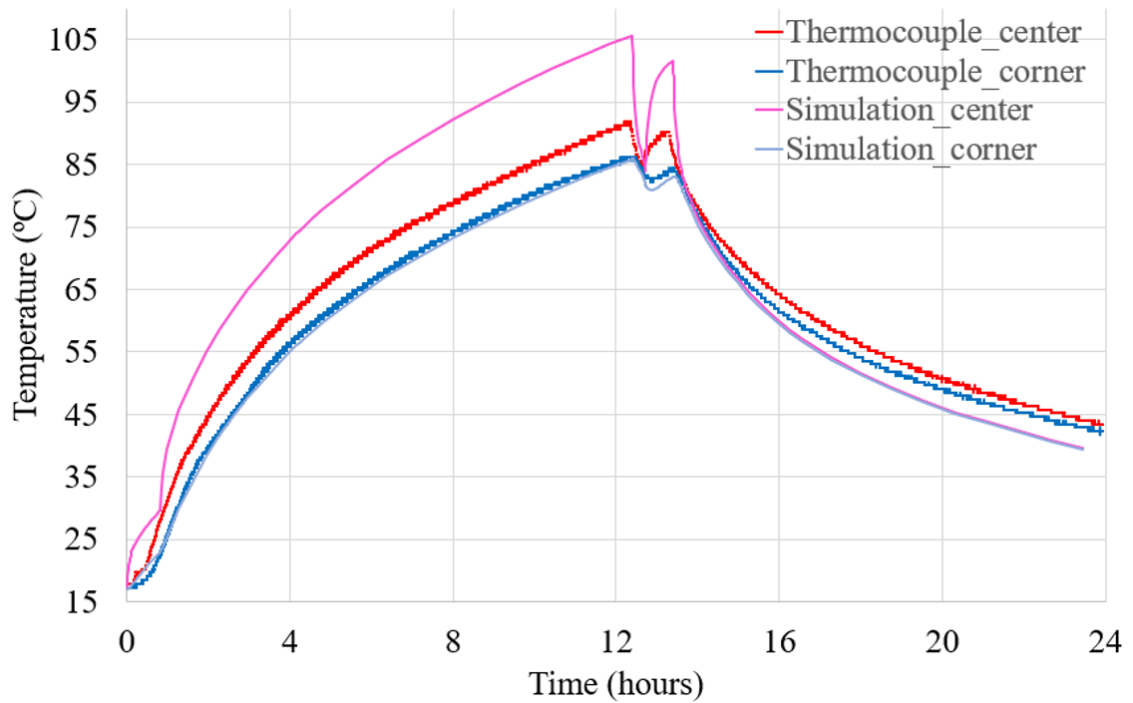


Figure 3.18 Graph showing the temperature evolution measured by the thermocouples vs the temperature simulated by the finite element simulation in the HRS dump..

data, as the overall thermal inertia of the system was much smaller.

3.5 Model extrapolation to higher energies and intensities

The same model that was adjusted for the test was used to extrapolate for higher energies and intensities. The FLUKA simulations include a model of target #650, the lightest target used in ISOLDE up to date. This target contains 14.85 grams of Multi-Walled Carbon Nanotubes (MWCNT) with a density of 0.5 g/cm³. The beam size is 3.5 mm sigma at the target. The temperature quoted is the maximum temperature in the dump in a steady-state, that is reached in general under 3 days of operation. The Von Mises stress quoted is found by starting with a steady-state thermal simulations, adding a transient thermal simulation of a single pulse, and exporting the temperatures to a transient structural simulation. The simulations were made for HRS, in which temperatures and stresses are higher. The results can be found in table 3.4.

3.6 Material limits

The uncertainty around the material grade and the structure of the dump (surface roughness, shape tolerances) makes it difficult to state any hard limits for safe operation. There is a lot of literature and material data about materials designed to operate at high temperatures (for example creep-resistant steels or austenitic alloys for use in boilers and pressure vessels). However, the dump blocks were mostly reused from past projects, therefore it cannot be assumed that they were chosen specifically to operate at high temperature. As a result, ‘normal’ alloys have to be considered, for which there is less data available at high temperature. In any case, the following points can be mentioned:

- Metals in general exhibit creep above 0.4 of their melting temperature, corresponding to 297 °C for cast iron and 408 °C for structural steel.
- Ductile cast irons retain relatively high tensile strengths (>400 MPa) up to 350 °C. However, above 400 °C creep behaviour starts to dominate, with significant creep appearing with stresses as low as 50 MPa, which will eventually lead to rupture [17].
- Suggested maximum temperatures for continuous service for carbon steels, based on creep or rupture data, is 450 °C [18].

3.7 Result discussion and conclusions

The dumps were installed in 1991, and their design does not reflect the best practices which are widely followed for beam-intercepting devices today: they are not cooled, they are not accessible for inspection or maintenance, the materials and boundary conditions are not clearly documented, they show signs of corrosion, and they lack any remote-handling capabilities. In addition, any problems requiring dump intervention would imply a time of at least a year to access the dumps. Despite the uncertainties introduced by the factors mentioned above, the simulations and measured data presented in this report and summarised in Table 3.4 show the following conclusions for different combinations of energy and intensity:

- 1.4 GeV / 3 µA or 2 GeV / 2 µA (green highlight): there should not be any catastrophic degradation of the condition of the blocks.
- 2 GeV at 6 µA or 13.4 µA (red highlight): not compatible with safe operation of the dump.
- 1.7 GeV / 3 µA or 2 GeV / 3 µA (no highlight): operation at these parameters could be authorized depending on the target selected and associated boundary conditions.

These conclusions are true provided that the assumptions mentioned in this report are maintained (in particular that a target with similar or superior density to #650 is installed in the front-end). Any increase of beam parameters must be accompanied by careful control of the maximum temperatures

Table 3.4 Results for different energies and intensities. See section 3.7 for more information.

Energy	Intensity	Max temperature in steady-state with lightest possible target inserted	Max VM stress
1.4 GeV	2 μ A	135 °C	51 MPa
1.4 GeV	3 μ A	199 °C	89 MPa
1.7 GeV	2 μ A	160 °C	63 MPa
1.7 GeV	3 μ A	239 °C	114 MPa
2.0 GeV	2 μ A	187 °C	77 MPa
2.0 GeV	3 μ A	280 °C	140 MPa
2.0 GeV	6 μ A	612 °C	-
2.0 GeV	13.4 μ A	1257 °C	-

measured by the thermocouples. If any of the thermocouples stopped working, they should be replaced at the earliest opportunity. ISOLDE operation with no target installed at higher energies or intensities (above 1.4 GeV / 2 μ A), such as potential future SEM grid tests, should be further evaluated from the perspective of the dump, as it is possible that an intensity limitation should be introduced for such tests.

4 Design and thermo-mechanical evaluation of the future dumps

This chapter proposes a new dump design to be manufactured and installed in the ISOLDE facility, including design constraints, beam parameters, design concept, and thermo-mechanical evaluation. The proposed new dump will be able to operate safely and reliably in the foreseeable future of the ISOLDE facility.

4.1 Design constraints

Any proposed dump design should comply with the following constraints:

- The new dumps will need to be installed in the same place where the current dumps are, with the corresponding constraints in terms of space and possible access.
- The dump design should be made with the goal of a dump lifetime of 25 to 30 years, therefore sufficient margin should be built into the design.
- Potential future optics changes must stay compliant with the beam dimensions limits on the dump as laid out in the beam specification document [19].
- The dump and its supports must be designed to ensure that the alignment with respect to the beam line can be both checked and adjusted.
- The dump design should be optimised to facilitate transport and handling, considering the increased activation of the dump through its lifetime. The dump and its shielding will be designed to be remote-handling compatible.
- The need for maintenance interventions must be reduced as much as possible – any consumable parts will be located far enough from the dump to allow exchange while respecting the ALARA (As Low As Reasonably Achievable) principle.
- The dump shielding should foresee the possibility to introduce a monitoring system to assess the visual status of the core (either via a periscope system or via the reservation of a path via the shielding to introduce an endoscope from the accessible area outside the shielding).
- The full lifecycle of the dump should be considered in the design, from installation to decommissioning at the end of its life, including potentially waste packaging.
- Monitoring of the dump cooling system, including flow, temperature and pressure should be included and made available to be connected to the interlock system.

4.1.1 Beam parameters

To comply with any possible scenario that might develop during the lifetime of the dump, the beam parameters have been conservatively estimated. They can be seen in table 4.1.

Table 4.1 Beam parameters for future dump design..

Parameter	Value
Beam energy	2.0 GeV
Max beam intensity	1×10^{14} ppp
Number of bunches	4
Bunch length	250 ns
Bunch spacing (center to center)	552 ns
Total pulse length	1906 ns
Repetition period	1.2 s
Beam intensity	13.4 μ A
Beam power	26.7 kW
Minimum beam size ($1\sigma, H \times V$)	$1.5 \times 1.5 \text{ mm}^2$
Nominal beam size ($1\sigma, H \times V$)	$4.8 \times 2.7 \text{ mm}^2$

The time structure of the beam is the one described in figure 2.2. The quoted beam sizes are specified on the dump upstream surface. The minimum beam size corresponds to an accident scenario: the worst possible configuration of the beam optics that results in the smallest possible beam size (which increases the power density and results in more challenging conditions for the dump). However, the beam size can be continuously monitored and it's extremely unlikely that operation with such a small beam size would happen for longer than a few seconds. For this reason, two different design scenarios were proposed, depending on the beam size (and thus beam power density) selected:

- Accident scenario beam size: 5 consecutive shots. It is assumed that an interlock will be installed, which will constantly monitor the beam size and stop the beam if the beam size is under a certain minimum 5 times in a row).
- Nominal beam size: steady-state plus one shot.

It has been found that the second scenario is the most restrictive in terms of thermo-mechanical load on the dump, and thus it will be the one considered in this document unless stated otherwise. For reference, the results for the first scenario are presented in section 4.6.3. The presence or not of the ISOLDE target upstream of the dump also has a huge impact on the energy profile that reaches the dump. The worst case scenario is that no ISOLDE target is installed, and thus this has been the conservative scenario considered for the design of the new dump. Nonetheless a simulation with a target has been performed and is presented in section 4.6.2.

4.2 Design concept

4.2.1 Early designs

The early designs were inspired by the proton synchrotron booster (PSB) dump [20], which was installed in 2013 with relatively similar beam parameters and requirements. It consisted of a 1500 mm-long, 400 mm-diameter Copper-Chromium-Zirconium (CuCr1Zr-UNS C18150 [21]) cylinder, with external fins to aid heat transfer via the forced air-cooling system.

The first design was a simple cylinder made of CuCr1Zr, 1500 mm-long and with a diameter of 400 mm-diameter. Two simulations were set up to evaluate the maximum temperature and stress on the CuCr1Zr. As can be seen in the first two rows of table 4.2, the temperatures and stresses were too high for reliable operation. Therefore, a graphite cylinder was introduced in the design. Different simulations were setup to see the impact of the length of the graphite. The diameter of the

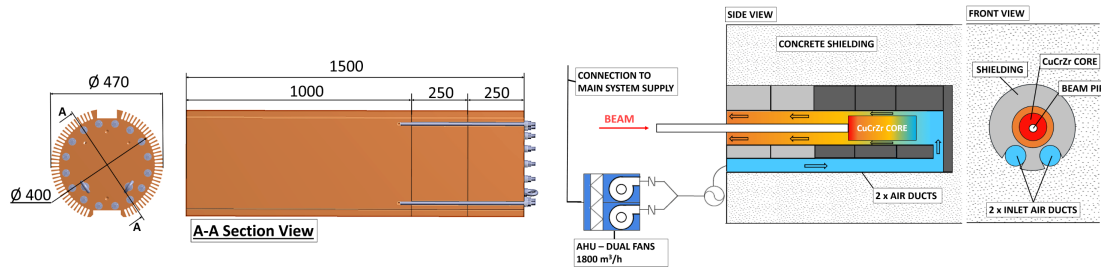


Figure 4.1 PSB dump. On the left the size and shape of the dump is shown, with dimensions in mm. On the right, a schematic shows how the dump was air-cooled.

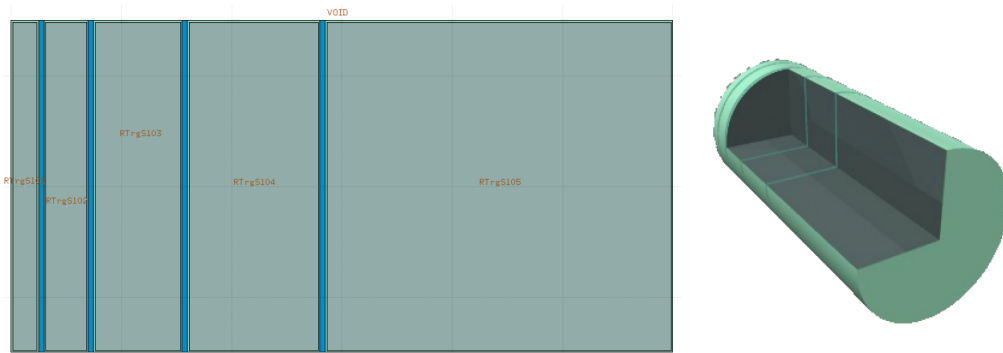


Figure 4.2 Preliminary model of the water-cooled, tantalum-cladded tungsten dump. In the image, the beam would come from the right.

graphite diluter was chosen to make sure that the beam will always impact the graphite first. The difference in length has a great effect on the temperature and stress on the CuCr1Zr. A balance on the length of the diluter needed to be found, as increasing the length diminished the stopping power of the dump, which would require to place additional shielding downstream of the dump.

In addition, a dump made of tungsten was also considered. The advantage of tungsten would be that the increased density would allow to reduce the overall length, from 1500 mm to 600 mm, which would increase the amount of shielding that can be placed around the dump. Based on existing experience with tungsten Beam Intercepting Devices [22], a concept was studied with a series of tungsten cylinders placed one after the other, with 5 mm gaps between them to allow for pressurized cooling water. To avoid direct contact between the water and the tungsten, which can lead to erosion, corrosion, and embrittlement [23], a 1.5 mm cladding of tantalum (Ta2.5W alloy) was added.

A FLUKA simulation was performed in order to verify its feasibility. It showed that the adiabatic

Table 4.2 Results of the early designs. The quoted maximum temperatures and stresses are for the CuCr1Zr. During the early designs the beam parameters were slightly different to the ones that were finally chosen.

Dump structure	Beam parameters	Max temperature	Max stress
Pure CuCr1Zr, $\varnothing 400$ mm, 1500 mm length	$1 \times 1 \text{ mm}^2$, 1 shot from 22 °C	969 °C	—
Pure CuCr1Zr, $\varnothing 400$ mm, 1500 mm length	$5 \times 2 \text{ mm}^2$, steady-state + 1 shot	219 °C	332 MPa
CuCr1Zr, $\varnothing 400$ mm, 1500 mm length	$1 \times 1 \text{ mm}^2$, 1 shot from 22 °C	254 °C	275 MPa
+ Graphite diluter $\varnothing 200$ mm, 300 mm length			
CuCr1Zr, $\varnothing 400$ mm, 1500 mm length	$1 \times 1 \text{ mm}^2$, 1 shot from 22 °C	49 °C	41 MPa
+ Graphite diluter $\varnothing 200$ mm, 600 mm length			

temperature increase from just a single pulse in the tungsten exceeded 360 °C. Even with pressurized water, this temperature increase would be enough to evaporate the cooling water. Therefore this concept was ruled out.

4.2.2 Hot Isostatic Pressing

Hot Isostatic Pressing (HIP) is a manufacturing process which compresses materials by applying high temperature (up to 2000 °C) and high isostatic gas pressure (up to 200 MPa). A brief explanation will be included due to its importance to the manufacturing of the proposed dump. HIP has been used mainly to heal casting or additive manufacturing defects and for powder metallurgy parts consolidations [24, 25, 26]. In the context of this work, HIP would be used to join the stainless-steel cooling pipes with the CuCr1Zr main dump. The process would require pressure hydrostatically applied both inside the pipes and outside the assembly, as well as high temperature during several hours. Following that, an additional thermal treatment is necessary to recuperate the thermal and mechanical properties of the CuCr1Zr. The advantage of using HIP would be that diffusion bonding would take place between the two materials, hence ensuring a perfect thermal bond. A previous study [27] shows the specific details of this methodology for the Super Proton Synchrotron internal beam dump. The study shows that the thermal conductivity at the interface between both materials is simply limited by the material with the lowest thermal conductivity. Similarly it shows that a diffusion bonded interface does not affect the mechanical strength.

4.2.3 Water-cooling vs gas-cooling

Given the design constraints, it was clear that the new dump would need to be actively cooled, with either water or gas (air or nitrogen). A pre-design was made for both concepts. The water-cooled concept had 8 pipes made of stainless steel, bonded to the CuCr1Zr, which would carry pressurised water. The air-cooled dump was a copy of the PSB dump previously mentioned, with a solid core and fins all along its length. However, a difference with respect to the PSB dump is that due to the geometry and access of the ISOLDE dump, an open system would not be possible. Therefore, a metal enclosure that surrounds the dump was drafted. The upstream face of the enclosure would be a beam window, meaning that the particle beam would traverse it and so would require additional calculations to ensure structural stability.

The basic cooling parameters for both concepts are shown in table 4.3.

Table 4.3 Cooling parameters comparison.

	Water cooling	Air cooling
Flow	1.76 kg/s	2500 Nm ³ /h (0.8975 kg/s)
Temperature delta	2.6 °C	21 °C
Dump pressure drop	60 kPa	5 kPa
Pipe internal diameter (dump inlet/outlet)	15 mm	134.5 mm
Flow average velocity (dump inlet/outlet)	10 m/s	49 m/s
Total power dissipated	19 kW	19 kW

In order to choose the different parameters, the starting points were the total power to be dissipated and the maximum flow velocities to be kept inside the pipes. From that data, a suitable compromise between pipe diameter, flow rate and temperature drop could be found.

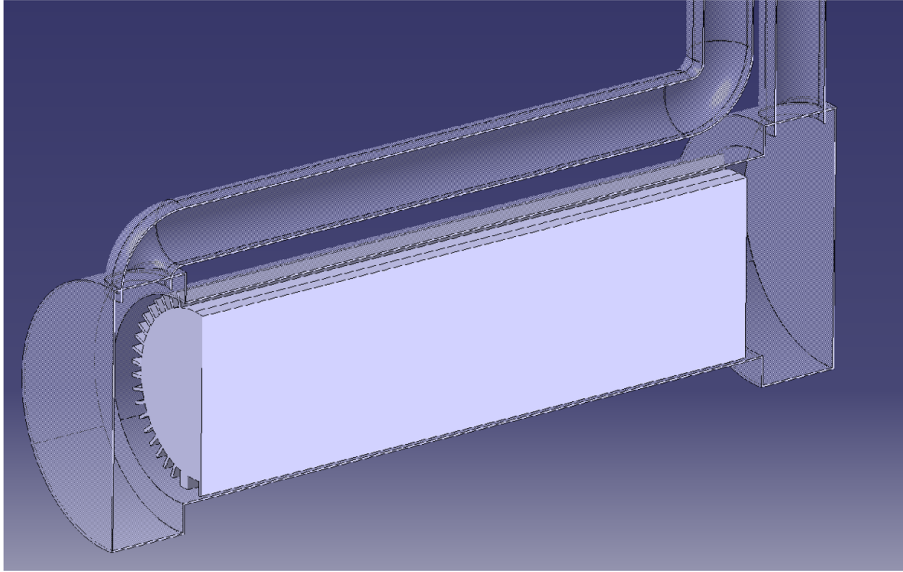


Figure 4.3 Half view of the air-cooled dump, including the outer enclosure with the inlet and outlet pipes, and the dump block with its cooling fins.

The total power corresponds to the beam power that is dissipated in the dump. The rest of the power, approximately 7.7 kW goes into the outer (not actively cooled) shielding (see section 4.6.1 for more details).

The results for the air-cooled version will be presented here, while the results for water-cooled model will be presented in sections 4.3 and 4.4.

Table 4.4 Air-cooling results.

Parameter	CuCr1Zr	Graphite (R4550)
Temperature (steady-state)	107 °C	135.3 °C
Temperature (steady-state + 1 shot)	119 °C	175.3 °C
Von Mises stress (safety factor)	24 MPa (10)	-
Christensen criteria (safety factor)	-	0.26 (3.8)

Table 4.5 Water-cooling results.

Parameter	CuCr1Zr	Graphite (R4550)
Temperature (steady-state)	62.3 °C	73.2 °C
Temperature (steady-state + 1 shot)	75.7 °C	118.8 °C
Von Mises stress (safety factor)	21 MPa (11)	-
Christensen criteria (safety factor)	-	0.27 (3.7)

As can be seen, the thermo-mechanical performance of both concepts was acceptable. Due to this, the decision was taken based on additional factors:

- Dump block feasibility in terms of thermo-mechanical simulations: both solutions were acceptable, however water-cooling had a higher safety margin.
- Dump manufacturing: the water-cooling solution requires a relatively complex pipe routing, plus an additional HIPping process. Meanwhile the air-cooled dump itself would be simpler

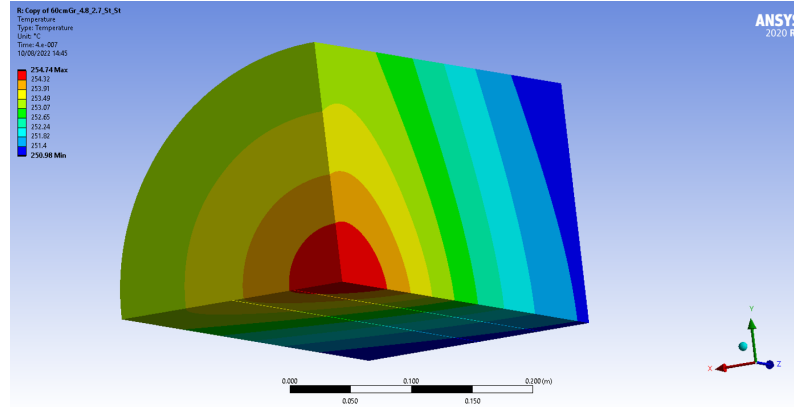


Figure 4.4 Quarter view of downstream section of a shorter actively cooled dump, showing the steady-state temperatures.

to manufacture, however it would require an additional enclosure, including a beam window and an air-tight interface between the enclosure and the dump itself.

- Coolant fluid leak detection: it would be easier to detect and control a water leak.
- Coolant leak prevention: the coolant pipes will potentially run in open air between the target area and the cooling station.
- Pipe diameter: water-cooling requires much smaller pipes, which are much easier to integrate and require less overall shielding. In particular, the vertical section of the air-cooling pipes would create a significant weakness in the shielding which would need to be compensated by additional shielding.
- Cooling station pressurization: for air-cooling, the entire volume of the cooling station would need to be under-pressurized.
- Cost/technical limitations from the point of view of the cooling station: the preliminary feedback from the Cooling and Ventilation expert was that water-cooling would be a more standard system and thus less risky.

4.2.4 Simulation with shorter dump

An additional idea that was studied was to make a shorter dump, or more precisely, to make the actively-cooled part of the dump shorter. Thus the upstream 1000 mm would remain actively cooled, and the downstream 500 mm would be a simple block of CuCr1Zr with no cooling. The advantage would be a smaller, more compact cooled dump, which would simplify the manufacturing and the overall assembly. A thermal simulation of the downstream block was performed with relatively conservative convection ($5 \text{ W/m}^2 \cdot \text{K}$ at 40°C , corresponding to stagnant air) applied around it. The results can be observed in figure 4.4. As it can be seen, the temperatures are quite high (255°C) and consequently this idea was dismissed.

4.2.5 Final conceptual design

The proposed dump geometry is a 1500 mm-long, 400 mm-diameter Copper-Chromium-Zirconium (CuCr1Zr-UNS C18150 [21]) cylinder, with a 600 mm-long, 200 mm-diameter graphite (isostatically pressed graphite [28]) cylinder which acts as a diluter. The length of the dump has been selected to contain most of the prompt radiation generated in the beam interaction process and minimize leaking of radiation downstream. The copper alloy has been selected due its high density, high thermal conductivity, and high strength. The diluter has been added as a direct beam impact on the copper alloy would have increased the temperatures close to the melting point; the graphite however can withstand a direct hit due its lower density and good mechanical properties. A series

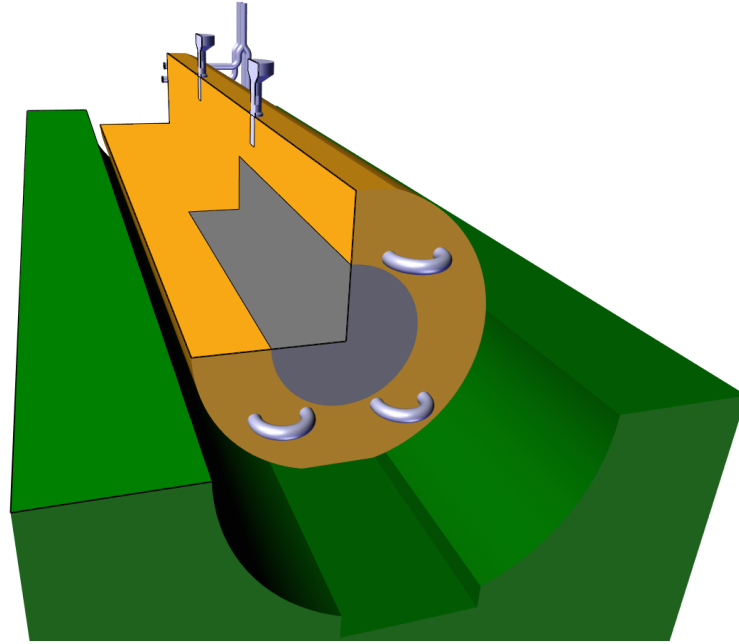


Figure 4.5 Quarter view of the new dump design.

of stainless-steel water-cooling pipes are inserted in the CuCr1Zr in order to cool it. The cooling pipes and the copper alloy assembly will be assembled using Hot Isostatic Pressing (HIP). The graphite diluter will be shrink-fitted into the copper alloy assembly.

Table 4.6 Material properties for the future dump design.

Material properties at 20 °C	CuCr1Zr	Graphite (R4550)	Stainless steel
Density	8.89 g/cm ³	1.83 g/cm ³	7.75 g/cm ³
Young Modulus	130 GPa	11.5 GPa	193 GPa
Poisson's ratio	0.3	0.14	0.31
Thermal conductivity	357 W/m·K	105 W/m·K	15 W/m·K
Specific heat capacity	393 J/kg·K	721 J/kg·K	480 J/kg·K

4.3 Finite element modelling

The simulation was setup using a similar approach to the one explained in the previous section: FLUKA Monte Carlo simulations [6] were used to calculate the energy deposited by the beam (see section 2.1 for details), and this energy was later imported into ANSYS[®] Mechanical[™][5] for thermo-mechanical finite element analysis.

The scenario considered for design was direct beam impact on the dump, with no target inserted, until a steady-state was reached. This scenario was simulated in ANSYS by turning the time integration off in the first time step. From that steady-state, an additional single pulse (composed of 4 bunches, figure 2.2) was simulated.

The thermal contact resistance between the CuCr1Zr and the cooling pipes was considered as zero due to the perfect bonding during the HIP process. The TCC between the CuCr1Zr and the graphite has been computed based on semi-empirical formulations [16], (see section 3.4.1) using the contact pressure derived from the shrink-fitting parameters. An independent static structural simulation was performed with a realistic (200 µm) interference fit, in order to get a realistic value (22 MPa) for the

contact pressure. It was verified that the effect of the shrink-fitting on both cylinders did not have significant adverse effects in terms of stress: the additional stress on the CuCr1Zr was relatively small and in different regions to beam-induced stress, and the graphite was in compression and thus exhibited a negative Christensen criterion. Nevertheless further simulations should be performed in order to estimate the variation of contact pressure at both extremes of the tolerances of the inner and outer cylinders, and possibly couple this shrink-fitting analysis with the beam-induced simulations.

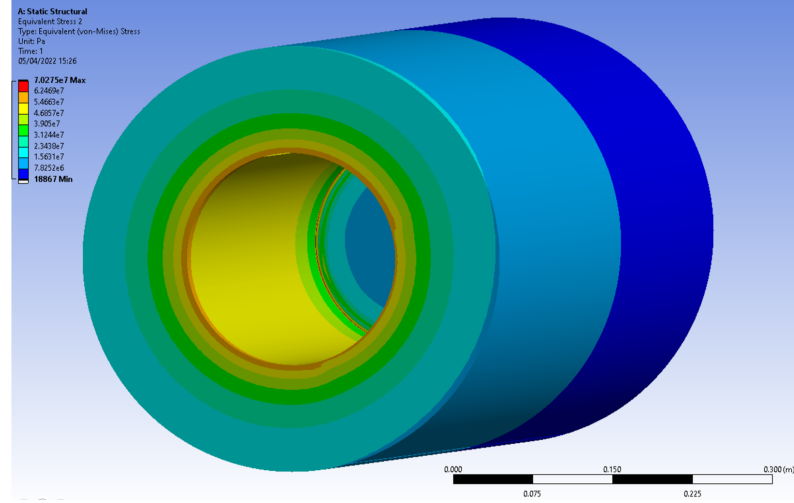


Figure 4.6 Von Mises stress results in the shrink-fitting FE model.

The HTC was calculated using the Dittus-Boelter equation [29] and additionally checked by running a simulation with ANSYS® FLUENT™.

$$Prandtl = \nu / \alpha$$

ν being the kinematic viscosity and α the thermal diffusivity.

For $Re > 10000$:

$$Nusselt = 0.023 * Re^{4/5} * Pr^{0.4}$$

$$h = Nu * \lambda / D$$

The actual values were the following:

Table 4.7 Final values for HTC calculation using the Dittus-Boelter equation.

Parameter	Value
Pipe diameter	15 mm
Mean speed of the flow	2.5 m/s
Reynolds number	46800
Prandtl number	5.4
Nusselt number	246
Convective coefficient	10000

4.4 Results

The temperature evolution in the dump in the first 4 ms can be observed in figure 4.7.

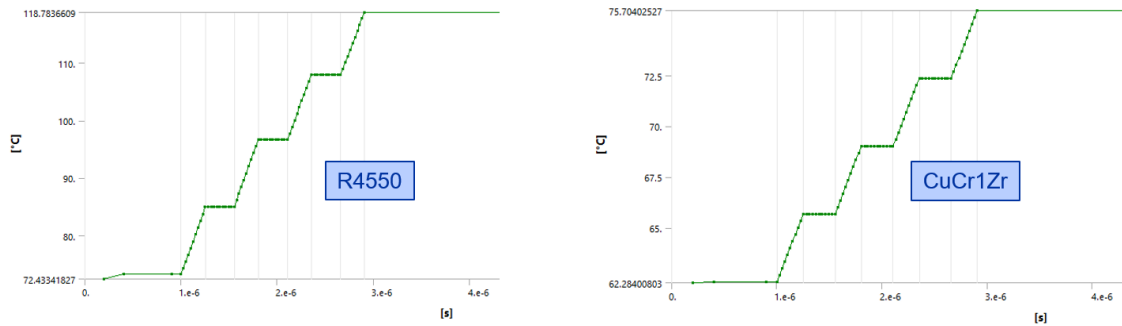


Figure 4.7 Temperature evolution on the graphite (left) and the CuCr1Zr (right) over the first 4 ms. The effect of the 4 particle bunches is clearly visible.

The resulting stress in the graphite is shown in figure 4.8. The failure criterion for the graphite was the Christensen criteria [7], using the material properties found in its datasheet [28].

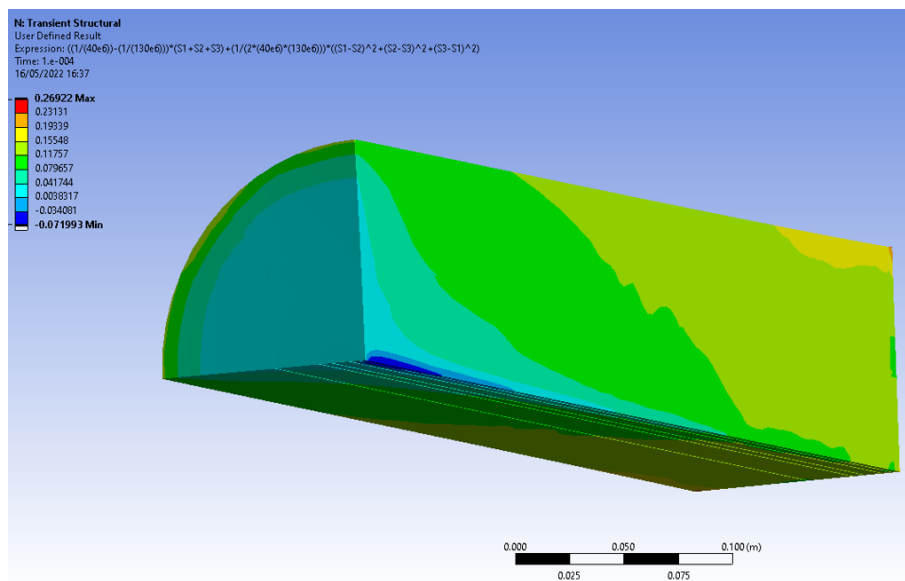


Figure 4.8 Christensen criterion for the graphite, with a maximum of 0.27.

The resulting stress in the CuCr1Zr is shown in figures 4.9 and 4.10. The failure criteria for the CuCr1Zr is the Von Mises criterion (based on a yield strength of the material of 230 MPa [20]).

The overall results are summed up in table 4.8.

Table 4.8 Thermo-mechanical results for the future dump design.

Parameter	CuCr1Zr	Graphite (R4550)
Temperature (steady-state + 1 shot)	75.7 °C	118.8 °C
Von Mises stress (safety factor)	21 MPa (11)	-
Christensen criteria (safety factor)	-	0.27 (3.7)

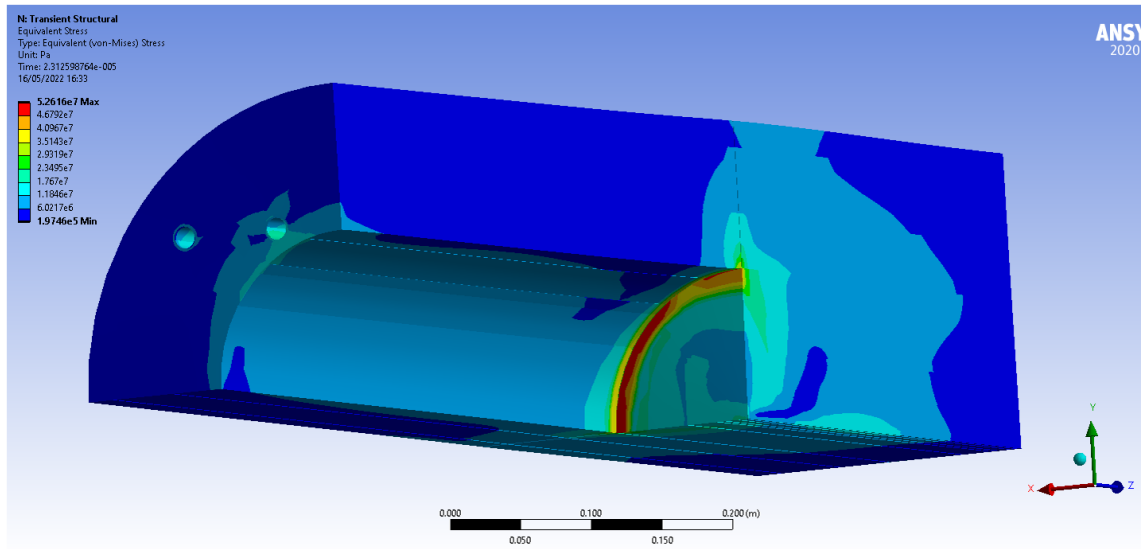


Figure 4.9 Von Mises stress in the CuCr1Zr, with a maximum of 53 MPa that is however heavily influenced by the local contact boundary conditions.

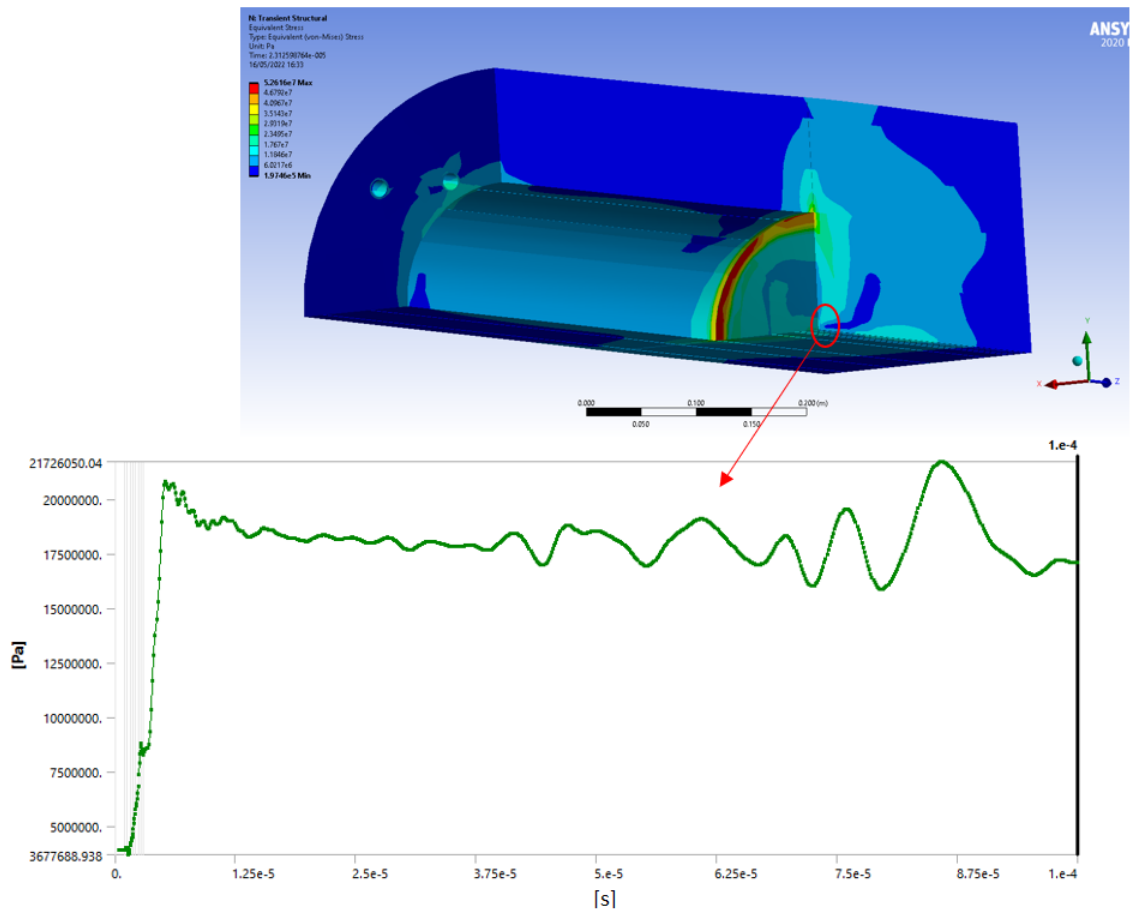


Figure 4.10 Von Mises stress in the center of the upstream face of the CuCr1Zr, with a maximum of 21 MPa.

4.5 Manufacturing notes

The proposed methodology to manufacture the dump would be the following:

- Procurement of the bulk materials.
- Machining of 3 separate CuCr1Zr blocks: a center section and upper and lower caps, including the straight slots for the stainless steel cooling pipes and the aperture for the graphite diluter.
- Bending of the cooling pipes.
- HIP process in order to bond together the three CuCr1Zr parts with the cooling pipes inside. This is a complex process involving several stages: preparation of the HIP capsule (a welded assembly containing the 3 CuCr1Zr parts and the pipes), verification of the leak tightness (as any air pockets trapped inside could be detrimental to the diffusion bonding process), the HIP process itself (with different stages at different pressures and temperatures), the capsule opening and testing to check any non-compliance, and finally the heat treatments in order to regain the mechanical and thermal properties that might have been degraded during the HIP process.
- Final machining of the graphite diluter hole, performed after the HIP process to avoid any deformation.
- Shrink-fitting of the graphite diluter into the overall assembly, aided by a small temperature increase ($<200\text{ }^{\circ}\text{C}$) of the CuCr1Zr assembly.
- Welding of the rest of the cooling pipes.

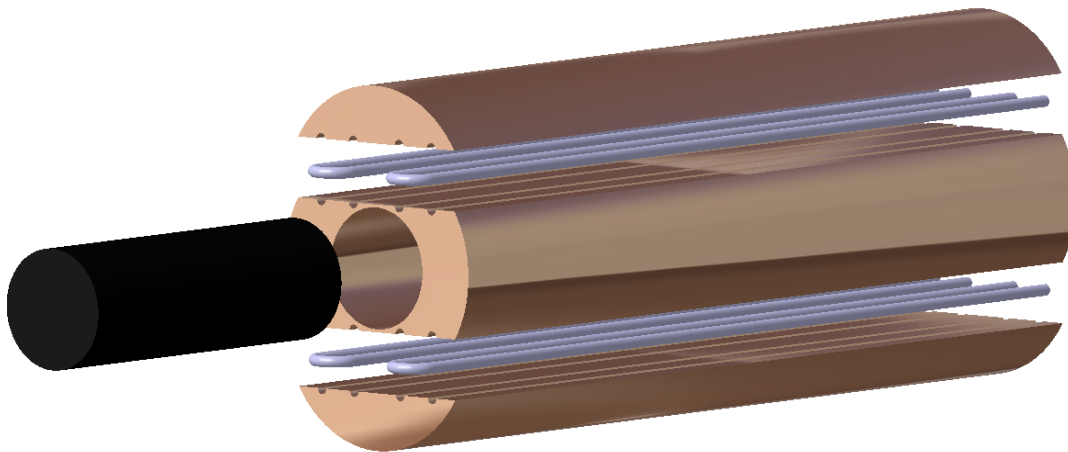


Figure 4.11 Schematic of the division for the dump manufacturing: first the three CuCr1Zr parts and the cooling pipes would go through the HIP process, and then the graphite diluter would be inserted.

4.6 Additional studies

4.6.1 Power deposition on the shielding

Although the main purpose of the dump is to contain the beam energy, it is unavoidable that a small proportion will escape downstream. FLUKA simulations showed that in this case the dump absorbs 72% of the beam energy, while the surrounding steel shielding absorbs the remaining 28% (9 kJ). A simulation was performed in order to ensure that this energy would not have adverse effects on the surrounding steel shielding, which is not actively cooled. A steady-state thermal simulation was setup assuming conservative cooling parameters for the shielding: a constant stagnant air convection

of $3 \text{ W}/\text{m}^2 \cdot \text{K}$ at 22°C . The results in figure 4.12 show an acceptable maximum temperature of 61°C in the shielding.

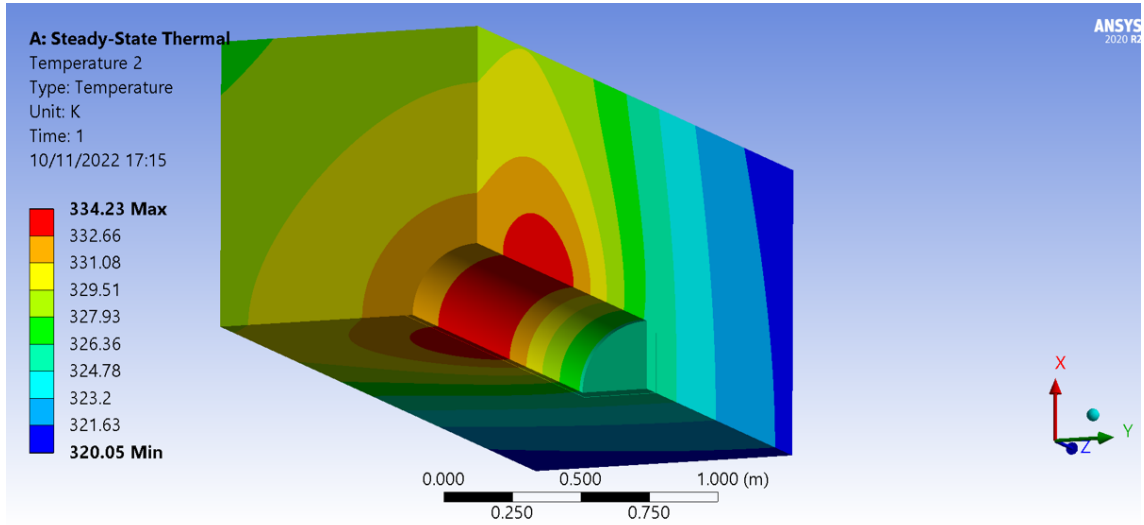


Figure 4.12 Temperature results (shown in Kelvin) of the simulation of the power deposition on the surrounding shielding.

4.6.2 Simulation with target installed

In order to provide an example of the usual operating conditions of the dump, a simulation was performed with a typical target inserted. The chosen example was a UC_4 target with 82.9% of U-238, 16.8% of C-12 and 0.2% of U-235, for a total mass of 7 g, contained in a graphite sleeve and tantalum container. Overall this is a much denser target than any others previously used in this work. A steady-state thermal simulation plus a single pulse was simulated, with an overall setup comparable to that shown in sections 4.3 and 4.4, with the difference being only the inclusion of a dense target. As it can be observed in figure 4.13 and table 4.9, there is a huge difference in the maximum temperatures that are reached. Nevertheless it's important to remember that the variety in ISOLDE targets is significant and will potentially become even bigger in the future, and the dump needs to withstand all possible scenarios.

Table 4.9 Thermal results of the proposed dump with a target installed.

Parameter	CuCr1Zr	Graphite (R4550)
Temperature (steady-state)	30.6°C	34.4°C
Temperature (steady-state + 1 shot)	30.7°C	34.7°C

4.6.3 Results for five consecutive beam shots

As mentioned in section 4.1.1, there is a second design scenario which was considered for the dump, consisting in a much smaller beam size (thus increasing the energy density over a smaller volume of the dump) during 5 consecutive pulses. The results of such scenario are shown in table 4.10. It can be verified that the thermo-mechanical load on the dump is much smaller than with the main design scenario.

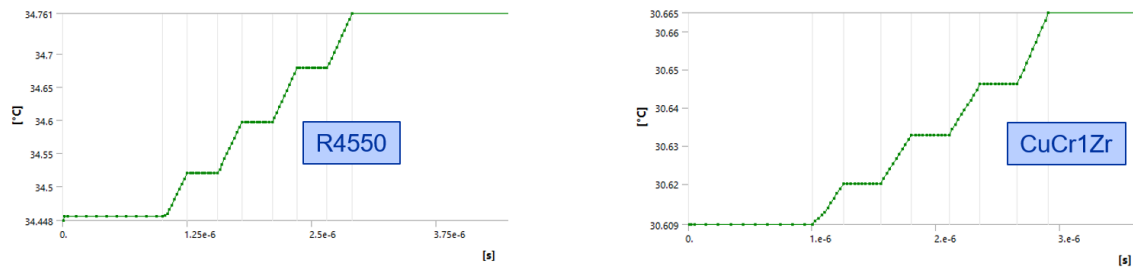


Figure 4.13 Temperature evolution on the graphite (left) and the CuCr1Zr (right) over the first 4 ms with a target installed.

Table 4.10 Thermo-mechanical results for the future dump design using the design scenario of 5 consecutive shots with the smallest (accident) beam size..

Parameter	CuCr1Zr	Graphite (R4550)
Max temperature after the 5th shot	51 °C	234 °C
Von Mises stress	35 MPa	-
Christensen criteria	-	0.06

5 Conclusions

The current operation of the ISOLDE beam dumps has been evaluated. The thermocouple installation and subsequent tests on the HRS and GPS dumps provided critical data to evaluate the thermo-mechanical behavior of these systems under operational conditions. The temperatures recorded during the tests will be compared later with finite element simulations to validate the accuracy of the thermal models. The thermocouples will remain active throughout the 2023 ISOLDE physics run, offering ongoing insights into the dumps' thermal performance.

In the thermo-mechanical evaluation, the geometry, materials, and boundary conditions of the dump blocks were meticulously analyzed. Recycled from previous CERN projects, these blocks were subjected to a detailed assessment despite some inconsistencies in the drawings and material uncertainties. Simulations considered both steel and cast iron as potential materials due to the lack of specific material information. Boundary conditions, such as fixed external temperatures and thermal contact conductance values, were established based on empirical formulations and practical observations. The comparison between simulated temperatures and actual thermocouple data indicated a close match, with deviations within 20%, affirming the model's reliability.

Extrapolating the model to higher energies and intensities provided further insights into the operational limits of the dumps. The simulations highlighted safe operational parameters and potential risks, such as catastrophic degradation at higher intensities. Despite the inherent uncertainties in material grades and conditions, the study concluded that under controlled beam parameters, the dumps could operate safely. However, the importance of ongoing temperature monitoring and prompt thermocouple replacement was emphasized to ensure continued safe operation, particularly at elevated energies and intensities.

A future dump design has been proposed, compatible with the expected future ISOLDE operation. The first step in the design was the definition of the constraints and objectives of the design, especially the beam parameters. This was not an easy task as it involves many different departments and points of view such as ISOLDE operation, dump alignment, transport constraints, or Radiation Protection.

Two primary cooling solutions were compared: air-cooled and water-cooled systems. Both air-cooled and water-cooled concepts showed acceptable thermo-mechanical performance. From a manufacturing and integration standpoint, the water-cooled dump is more complex due to the intricate pipe routing and additional Hot Isostatic Pressing (HIP) process. Conversely, the air-cooled dump, although simpler in its core, requires a complex outer enclosure and additional components to ensure airtightness and structural integrity. The water-cooled system benefits from smaller pipe diameters, which ease integration and reduce the need for extensive shielding, a significant advantage in maintaining overall structural efficiency and minimizing material costs.

Operational considerations also favored water cooling, which offers more straightforward coolant leak detection and prevention mechanisms, an essential factor in maintaining operational safety and reliability. Additionally, the water-cooling station, being a more standard system, presents fewer

technical risks and is favored by cooling and ventilation experts. Due to all of these factors, the water-cooling solution was ultimately selected.

Several design variations were considered, such as different geometries or materials. However, all of them were discarded for different motives which are explained for each case but that can be summed up as excessively high temperatures.

The final design features a 1500 mm-long CuCr1Zr cylinder with an integrated 600 mm-long graphite diluter, effectively balancing thermal conductivity, mechanical strength, and radiation containment.

Advanced simulations using FLUKA Monte Carlo and ANSYS® Mechanical™ provided detailed insights into the thermal and stress distributions under various operating conditions. These simulations validated the robustness of the selected water-cooled design. Contact pressures and heat transfer coefficients were calculated, ensuring the model's accuracy in predicting real-world performance.

The basic manufacturing process has been studied and involves precise machining, bending, HIP, and shrink-fitting procedures, ensuring high-quality assembly and optimal performance of the dump. Final machining and assembly steps are crucial for achieving the desired mechanical properties and ensuring the longevity of the dump under continuous operational stresses.

This work is not meant as a final dump design, and the proposed solution should be further evaluated in terms of fatigue strength, ease of manufacture, handling, and instrumentation.

In conclusion, the comprehensive evaluation of the cooling options and detailed thermo-mechanical simulations have led to the selection of a water-cooled dump design. This design not only meets the thermal and mechanical requirements but also addresses manufacturing and operational considerations effectively. The iterative approach of simulations and practical evaluations ensures that the future dumps will be both efficient in performance and reliable in long-term operation, making them well-suited for their intended application in beam energy dissipation and radiation containment.

Appendix A

APDL input file

All the simulations described in this work have been performed using the ANSYS® Workbench. However, the APDL code for one of the simulations has been included here for reference. In particular the code corresponds to a transient thermal simulation (see section 2.3 for details) of the future dump (see sections 4.3 and 4.4 for details and results).

The code has been edited for brevity, deleting the repetitive lines (lists of nodes or elements, definition of temperature-dependent properties, multiple similar contacts, etc) and adding empty lines to improve readability.

A.1 APDL code

```
/batch
/config,noelddb,1    ! force off writing results to database
*get,_wallstrt,active,,time,wall
! ANSYS input file written by Workbench version 2022 R2
! File used for geometry attach: D:\quarter_model_N\model_files\dp0\SYS
-15\DM\SYS-15.agdb
/title,model--Transient Thermal (G5)
! ***** Begin Custom Load Command Snippet *****
/COM, ACT Extensions:
/COM,    FlukaV1_Beta, 1.0
/COM,    688f3d8d-13cd-4193-a95a-6b7aac8b803e, xml
/COM,/COM,    LSDYNA, 2022.2
/COM,    5f463412-bd3e-484b-87e7-cbc0a665e474, wbex
/COM,/COM,    ANSYSMotion, 2022.2
/COM,    20180725-3f81-49eb-9f31-41364844c769, wbex
/COM,
! ***** End Custom Load Command Snippet *****

*DIM,_wb_ProjectScratch_dir,string,248
_wb_ProjectScratch_dir(1) = 'D:\quarter_model_N\model_files\dp0\SYS-15\
MECH\'
*DIM,_wb_SolverFiles_dir,string,248
_wb_SolverFiles_dir(1) = 'D:\quarter_model_N\model_files\dp0\SYS-15\MECH
\'
```

```

*DIM,_wb_userfiles_dir,string,248
_wb_userfiles_dir(1) = 'D:\quarter_model_N\model_files\user_files\'
/com,--- Data in consistent MKS units. See Solving Units in the help
      system for more information.
/units,MKS
/nopr
/wb,file,start          ! signify a WB generated input file
/prep7
! Turn off shape checking because checks already performed inside WB
  mesher.
! See help system for more information.
SHPP,OFF,,NOWARN
/nolist
etcon,set              ! allow ANSYS to choose best KEYOP's for 180x
  elements, resets any applicable keyopt to MAPDL defaults

/com,***** Nodes for the whole assembly *****
nblock,3,,198299
(1i9,3e20.9e3)
      1      5.307522511E-02      9.601150788E-02      9.963711899E-01
      (...)
      229142      1.020484721E-02      9.947794275E-02      0.000000000E+00
-1

/wb,elem,start          ! set before creation of elements
/com,***** Elements for Body 1 "Solid" *****
et,1,278
eblock,19,solid,,508
(19i9)
      1      1      1      1      0      0      0      0
      8      0      1      260      1406      771      265      261
      1279      269      266
      1      1      1      1      0      0      0      0
      8      0      508      642      902      1536      901      772
      1407      1408      773
-1
(...)
!Material Id = {C1D32ED0-F2DA-457F-8272-2F597D00A6F7}
/com,***** Elements for Body 72 "Solid" *****
et,72,278
eblock,19,solid,,3738
(19i9)
      72      72      20      72      0      0      0      0
      8      0      149975      37745      45261      43555      45712      45267
      45255      40914      45276
      72      72      20      72      0      0      0      0
      8      0      153712      29644      37130      35982      37735      44702
      45138      42499      45834
-1

```

```

!Material Id = {6A1981E7-87F2-4474-A806-5254AF92F35F}
/wb,elem,end          ! done creating elements

/com,***** Send User Defined Coordinate System(s) *****
local,12,1,0.,0.,0.,0.,0.
csys,0
toffst,273.15, ! Temperature offset from absolute zero

/wb,mat,start          ! starting to send materials
/com,***** Send Materials *****
Temperature = 'TEMP' ! Temperature
MP,DENS,1,7750, ! kg m-3
MP,ALPX,1,1.7e-05, ! C-1
MP,C,1,480, ! J kg-1 C-1
MP,KXX,1,15.1, ! W m-1 C-1
MP,RSVX,1,7.7e-07, ! kg m3 A-2 s-3
MP,EX,1,193000000000, ! Pa
MP,NUXY,1,0.31,
MP,MURX,1,1,
MP,UVID,1,d9ad4725-16e1-48de-a6c2-fd21089e23ba
MP,UMID,1,a172f1c0-b9bf-4419-af0a-0f896f0af551

(...)

TB,BISO,72,6,
TBTEMP,19.85
TBDATA,1,291000000,0
TBTEMP,99.85
TBDATA,1,273000000,0
TBTEMP,179.85
TBDATA,1,256000000,0
TBTEMP,259.85
TBDATA,1,238000000,0
TBTEMP,339.85
TBDATA,1,221000000,0
TBTEMP,499.85
TBDATA,1,186000000,0
MP,UVID,72,19e9e360-2e3e-478a-84d5-a5997de3f27c

/wb,mat,end          ! done sending materials

! ***** Begin Command Snippet *****
*dim,matids,,1
*set,matids(1),1
*set,matid,1
*dim,typeids,,1
*set,typeids(1),1
*DIME,inner_table,106100,1,1,ELEM,
*DIME,inner_table_aux,106100,1,1,ELEM,
inner_table(1,0,1) = 3811

```

```

inner_table(1,1,1) = 6.058970594983250e+13
(...)
inner_table(106100,0,1) = 210423
inner_table(106100,1,1) = 1.760531976010840e+11
CMBLOCK,inner_table_selection,ELEM,106100
(8i10)
      3811      3812      3813      3814      3815      3816      3817
      3818
      (...)
      210420      210421      210422      210423

*set, matids, ,
*set, typeids, ,
! ***** End Command Snippet *****

! ***** Begin Command Snippet *****
*dim,matids,,1
*set,matids(1),1
*set,matid,1
*dim,typeids,,1
*set,typeids(1),1
*DIME,outer_table,TABLE,51532,1,1,ELEM,
*DIME,outer_table_aux,TABLE,51532,1,1,ELEM,
outer_table(1,0,1) = 1
outer_table(1,1,1) = 1.767418784870560e+10
(...)
outer_table(51532,0,1) = 201434
outer_table(51532,1,1) = 4.560923855367610e+10
CMBLOCK,outer_table_selection,ELEM,51532
(8i10)
      1          2          3          4          5          6          7          8
      (...)
      201431      201432      201433      201434

*set, matids, ,
*set, typeids, ,
! ***** End Command Snippet *****

!***** Model Summary *****
!Solid, Stainless Steel, matid, 1
!Solid, Stainless Steel, matid, 2
!Solid, Stainless Steel, matid, 3
!Solid, Stainless Steel, matid, 4
!Solid, Stainless Steel, matid, 5
!Solid, Stainless Steel, matid, 6
!Solid, Stainless Steel, matid, 7
!Solid, Stainless Steel, matid, 8
!Solid, R4550 Graphite, matid, 9
!Solid, R4550 Graphite, matid, 10
!Solid, R4550 Graphite, matid, 11

```

```
!Solid, R4550 Graphite, matid, 12
!Solid, R4550 Graphite, matid, 13
!Solid, R4550 Graphite, matid, 14
!Gr_beam, R4550 Graphite, matid, 15
!Solid, R4550 Graphite, matid, 16
!Solid, R4550 Graphite, matid, 17
!Solid, R4550 Graphite, matid, 18
!Solid, R4550 Graphite, matid, 19
!Solid, CuCrZr, matid, 20
!Solid, CuCrZr, matid, 21
!Solid, CuCrZr, matid, 22
!Solid, CuCrZr, matid, 23
!Solid, CuCrZr, matid, 24
!Solid, CuCrZr, matid, 25
!Solid, CuCrZr, matid, 26
!Solid, CuCrZr, matid, 27
!Solid, CuCrZr, matid, 28
!Solid, CuCrZr, matid, 29
!Solid, CuCrZr, matid, 30
!Solid, CuCrZr, matid, 31
!Solid, CuCrZr, matid, 32
!Solid, CuCrZr, matid, 33
!Solid, CuCrZr, matid, 34
!Solid, CuCrZr, matid, 35
!Solid, CuCrZr, matid, 36
!Solid, CuCrZr, matid, 37
!Solid, CuCrZr, matid, 38
!Solid, CuCrZr, matid, 39
!Solid, CuCrZr, matid, 40
!Solid, CuCrZr, matid, 41
!Solid, CuCrZr, matid, 42
!Solid, CuCrZr, matid, 43
!Solid, CuCrZr, matid, 44
!Solid, CuCrZr, matid, 45
!Solid, CuCrZr, matid, 46
!Solid, CuCrZr, matid, 47
!Solid, CuCrZr, matid, 48
!Solid, CuCrZr, matid, 49
!Solid, CuCrZr, matid, 50
!Solid, CuCrZr, matid, 51
!Solid, CuCrZr, matid, 52
!Solid, CuCrZr, matid, 53
!Solid, CuCrZr, matid, 54
!Solid, CuCrZr, matid, 55
!Solid, CuCrZr, matid, 56
!Solid, CuCrZr, matid, 57
!Solid, CuCrZr, matid, 58
!Solid, CuCrZr, matid, 59
!Solid, CuCrZr, matid, 60
!Solid, CuCrZr, matid, 61
```

```

!Solid, CuCrZr, matid, 62
!Solid, CuCrZr, matid, 63
!Solid, CuCrZr, matid, 64
!Solid, CuCrZr, matid, 65
!Solid, CuCrZr, matid, 66
!Solid, CuCrZr, matid, 67
!Solid, CuCrZr, matid, 68
!Solid, CuCrZr, matid, 69
!Solid, CuCrZr, matid, 70
!Solid, CuCrZr, matid, 71
!Solid, CuCrZr, matid, 72
!***** End Model Summary *****
! get the diagonal of the bounding box. Needed later for other things
*get,_xmin,node,,mnloc,x
*get,_ymin,node,,mnloc,y
*get,_zmin,node,,mnloc,z
*get,_xmax,node,,mxloc,x
*get,_ymax,node,,mxloc,y
*get,_zmax,node,,mxloc,z
_ASMDIAG=(_xmax-_xmin)*(_xmax-_xmin)+(_ymax-_ymin)*(_ymax-_ymin)+(_zmax
-_zmin)*(_zmax-_zmin)
_ASMDIAG=SQRT(_ASMDIAG)

/wb,contact,start      ! starting to send contact
/com,***** Create Contact "pipeCu 1" *****
/com,                Real Constant Set For Above Contact Is 74 & 73
*set,tid,74
*set,cid,73
r,tid
r,cid
et,tid,170
et,cid,174
eblock,10,,208
(15i9)
    298272      74      74      74      0      1407      902      1536
    1408
(...)
    299399      74      73      74      0      56465      56464      58065
    57884
-1
keyo,cid,8,2          ! auto create asymmetric contact (from Program
    Controlled setting)
keyo,cid,10,0         ! adjust contact stiffness each NR iteration (
    from Program Controlled setting)
keyo,cid,12,5         ! bonded always
keyo,cid,18,1         ! small sliding turned on by application
keyo,cid,2,0          ! augmented Lagrange (from Program Controlled
    setting)

```



```

keyo,cid,4,0      ! on Gauss point (from Program Controlled
    setting)
keyo,cid,9,1      ! ignore initial gaps/penetration
keyo,cid,7,0      ! No Prediction
rmod,tid,3,10.    ! FKN
rmod,tid,5,0.     ! ICONT
rmod,tid,6,0.     ! PINB
rmod,tid,10,0.    ! CNOF
rmod,tid,12,0.    ! FKT
rmod,tid,36,999   ! WB DSID
rmod,cid,3,10.    ! FKN
rmod,cid,5,0.     ! ICONT
rmod,cid,6,0.     ! PINB
rmod,cid,10,0.    ! CNOF
rmod,cid,12,0.    ! FKT
rmod,cid,36,999   ! WB DSID
*set,_maxkxx,3572900.
rmod,cid,14,_maxkxx/_ASMDIAG    ! TCC, Divide by Length since Traction
    Based
rmod,tid,14,_maxkxx/_ASMDIAG    ! TCC, Divide by Length since Traction
    Based
keyo,cid,1,2      ! Pure thermal contact

(...)

/com,***** Create Contact "pipeCu 16" *****
/com,              Real Constant Set For Above Contact Is 136 & 135
*set,tid,136
*set,cid,135
r,tid
r,cid
et,tid,170
et,cid,174
eblock,10,,,308
(15i9)
    328726      136      136      136      0      6909      7300      6915
    6910
(...)
    330413      136      135      136      0      69743      66114      66248
    70144
-1
keyo,cid,8,2      ! auto create asymmetric contact (from Program
    Controlled setting)
keyo,cid,10,0     ! adjust contact stiffness each NR iteration (
    from Program Controlled setting)
keyo,cid,12,5     ! bonded always
keyo,cid,18,1     ! small sliding turned on by application
keyo,cid,2,0      ! augmented Lagrange (from Program Controlled
    setting)

```

```

keyo,cid,4,0          ! on Gauss point (from Program Controlled
    setting)
keyo,cid,9,1          ! ignore initial gaps/penetration
keyo,cid,7,0          ! No Prediction
rmod,tid,3,10.        ! FKN
rmod,tid,5,0.         ! ICONT
rmod,tid,6,0.         ! PINB
rmod,tid,10,0.        ! CNOF
rmod,tid,12,0.        ! FKT
rmod,tid,36,1433      ! WB DSID
rmod,cid,3,10.        ! FKN
rmod,cid,5,0.         ! ICONT
rmod,cid,6,0.         ! PINB
rmod,cid,10,0.        ! CNOF
rmod,cid,12,0.        ! FKT
rmod,cid,36,1433      ! WB DSID
*set,_maxkxx,3572900.
rmod,cid,14,_maxkxx/_ASMDIAG    ! TCC, Divide by Length since Traction
    Based
rmod,tid,14,_maxkxx/_ASMDIAG    ! TCC, Divide by Length since Traction
    Based
keyo,cid,1,2          ! Pure thermal contact
nsel,all
esel,all
/wb,contact,end      ! done creating contacts

/com,***** Send Named Selection as Element Component *****
esel,s,type,,9
esel,a,type,,10,19
esel,a,type,,21
esel,a,type,,24
esel,a,type,,41
esel,a,type,,65,72
cm,INNER_SECTION,elem
esel,all
/com,***** Send Named Selection as Element Component *****
esel,s,type,,1
esel,a,type,,2,8
esel,a,type,,20
esel,a,type,,22,23
esel,a,type,,25,40
esel,a,type,,42,64
cm,OUTER_SECTION,elem
esel,all
/golist
/wb,load,start        ! starting to send loads
fcum,add              ! add nodal forces up (needed in case have
    loads on the same edge,vertex)

```

```

fcum                ! reset default on fcum command since done
    sending WB F loads
/com,***** Create "Convection" *****
et,137,152
eblock,10,,,3810
(15i9)
    330414      137      137      137      0      4609      4105      4102
    4101
(...)
    334223      137      137      137      0      2685      129      130
    2556
-1
esel,s,type,,137
keyop,137,8,2.
keyop,137,13,0
esel,all
/com,***** Define Uniform Initial temperature
*****
tunif,22.
/gst,on,on
fini
*get,_numnode,node,0,count
*get,_numelem,elem,0,count
*get,_MAXELEMNUM, elem, 0, NUM, MAX
*get,_MAXNODENUM, node, 0, NUM, MAX
*get,_MAXELEMTYPE, etyp, 0, NUM, MAX
*get,_MAXREALCONST, rcon, 0, NUM, MAX
/go
/wb,load,end        ! done creating loads
/com,--- Number of total nodes = %_numnode%
/com,--- Number of contact elements = 35952
/com,--- Number of spring elements = 0
/com,--- Number of bearing elements = 0
/com,--- Number of solid elements = 157632
/com,--- Number of condensed parts = 0
/com,--- Number of total elements = %_numelem%
*get,_wallbsol,active,,time,wall

/com,*****
/com,***** SOLUTION *****
/com,*****
/solu
antype,4            ! transient analysis
kbc,1               ! stepped BC's
!eqsl,sparse        ! using sparse solver which is default so no
    eqsl command needed
cntr,print,1        ! print out contact info and also make no
    initial contact an error
rescontrol,,none    ! Do not keep any restart files
dmpoption,emat,no   ! Don't combine emat file for DANSYS

```

```

dmpoption,esav,no          ! Don't combine esav file for DANSYS
thopt,quasi,5.e-002
nlhist,nsol,MAX_TEMP,temp,max
nlhist,nsol,MIN_TEMP,temp,min
/com,***** Initial Time Increment Check And Fourier Modulus
*****
/com, Specified Initial Time Increment: 2e-07
/com, Estimated Increment Needed, le*le/alpha, Body 1: 3.65104
/com, Estimated Increment Needed, le*le/alpha, Body 2: 3.25752
/com, Estimated Increment Needed, le*le/alpha, Body 3: 3.98698
/com, Estimated Increment Needed, le*le/alpha, Body 4: 3.3398
/com, Estimated Increment Needed, le*le/alpha, Body 5: 3.6124
/com, Estimated Increment Needed, le*le/alpha, Body 6: 3.45137
/com, Estimated Increment Needed, le*le/alpha, Body 7: 3.6977
/com, Estimated Increment Needed, le*le/alpha, Body 8: 3.42895
/com, Estimated Increment Needed, le*le/alpha, Body 9: 0.224057
/com, Estimated Increment Needed, le*le/alpha, Body 10: 0.56948
/com, Estimated Increment Needed, le*le/alpha, Body 11: 0.537744
/com, Estimated Increment Needed, le*le/alpha, Body 12: 0.0771883
/com, Estimated Increment Needed, le*le/alpha, Body 13: 0.0525408
/com, Estimated Increment Needed, le*le/alpha, Body 14: 0.0214703
/com, Estimated Increment Needed, le*le/alpha, Body 15: 0.0130382
/com, Estimated Increment Needed, le*le/alpha, Body 16: 0.0214703
/com, Estimated Increment Needed, le*le/alpha, Body 17: 0.0525408
/com, Estimated Increment Needed, le*le/alpha, Body 18: 0.0771883
/com, Estimated Increment Needed, le*le/alpha, Body 19: 0.224057
/com, Estimated Increment Needed, le*le/alpha, Body 20: 0.785457
/com, Estimated Increment Needed, le*le/alpha, Body 21: 0.436593
/com, Estimated Increment Needed, le*le/alpha, Body 22: 0.587948
/com, Estimated Increment Needed, le*le/alpha, Body 23: 0.803092
/com, Estimated Increment Needed, le*le/alpha, Body 24: 0.18192
/com, Estimated Increment Needed, le*le/alpha, Body 25: 0.600109
/com, Estimated Increment Needed, le*le/alpha, Body 26: 0.819698
/com, Estimated Increment Needed, le*le/alpha, Body 27: 0.801698
/com, Estimated Increment Needed, le*le/alpha, Body 28: 0.289239
/com, Estimated Increment Needed, le*le/alpha, Body 29: 0.756526
/com, Estimated Increment Needed, le*le/alpha, Body 30: 0.739913
/com, Estimated Increment Needed, le*le/alpha, Body 31: 1.05967
/com, Estimated Increment Needed, le*le/alpha, Body 32: 1.08347
/com, Estimated Increment Needed, le*le/alpha, Body 33: 0.793216
/com, Estimated Increment Needed, le*le/alpha, Body 34: 0.635098
/com, Estimated Increment Needed, le*le/alpha, Body 35: 0.315417
/com, Estimated Increment Needed, le*le/alpha, Body 36: 0.57568
/com, Estimated Increment Needed, le*le/alpha, Body 37: 0.302625
/com, Estimated Increment Needed, le*le/alpha, Body 38: 0.235709
/com, Estimated Increment Needed, le*le/alpha, Body 39: 0.214744
/com, Estimated Increment Needed, le*le/alpha, Body 40: 0.223598
/com, Estimated Increment Needed, le*le/alpha, Body 41: 0.368506
/com, Estimated Increment Needed, le*le/alpha, Body 42: 0.27803
/com, Estimated Increment Needed, le*le/alpha, Body 43: 0.281942

```

```

/com, Estimated Increment Needed, le*le/alpha, Body 44: 0.586485
/com, Estimated Increment Needed, le*le/alpha, Body 45: 0.801093
/com, Estimated Increment Needed, le*le/alpha, Body 46: 0.783501
/com, Estimated Increment Needed, le*le/alpha, Body 47: 0.598615
/com, Estimated Increment Needed, le*le/alpha, Body 48: 0.817658
/com, Estimated Increment Needed, le*le/alpha, Body 49: 0.799702
/com, Estimated Increment Needed, le*le/alpha, Body 50: 0.288519
/com, Estimated Increment Needed, le*le/alpha, Body 51: 0.754643
/com, Estimated Increment Needed, le*le/alpha, Body 52: 0.738071
/com, Estimated Increment Needed, le*le/alpha, Body 53: 0.791241
/com, Estimated Increment Needed, le*le/alpha, Body 54: 1.08077
/com, Estimated Increment Needed, le*le/alpha, Body 55: 1.05704
/com, Estimated Increment Needed, le*le/alpha, Body 56: 0.574247
/com, Estimated Increment Needed, le*le/alpha, Body 57: 0.314632
/com, Estimated Increment Needed, le*le/alpha, Body 58: 0.633517
/com, Estimated Increment Needed, le*le/alpha, Body 59: 0.277338
/com, Estimated Increment Needed, le*le/alpha, Body 60: 0.301872
/com, Estimated Increment Needed, le*le/alpha, Body 61: 0.28124
/com, Estimated Increment Needed, le*le/alpha, Body 62: 0.235121
/com, Estimated Increment Needed, le*le/alpha, Body 63: 0.21421
/com, Estimated Increment Needed, le*le/alpha, Body 64: 0.223041
/com, Estimated Increment Needed, le*le/alpha, Body 65: 0.0626717
/com, Estimated Increment Needed, le*le/alpha, Body 66: 0.0105862
/com, Estimated Increment Needed, le*le/alpha, Body 67: 0.0174324
/com, Estimated Increment Needed, le*le/alpha, Body 68: 0.0426596
/com, Estimated Increment Needed, le*le/alpha, Body 69: 0.0174324
/com, Estimated Increment Needed, le*le/alpha, Body 70: 0.0426596
/com, Estimated Increment Needed, le*le/alpha, Body 71: 0.0626717
/com, Estimated Increment Needed, le*le/alpha, Body 72: 0.18192
/com,*****
/com,***** SOLVE FOR LS 1 OF 9 *****
esel,s,type,,137
nsle
sf,all,conv,10000.,28.
nsel,all
esel,all
/nopr
/gopr
autots,on          ! User turned on automatic time stepping
nsub,5,10,2,OFF
time,1.e-006
timint,off        ! Turn off time integration effects
outres,erase
outres,all,none
outres,nsol,all
outres,rsol,all
outres,eangl,all
outres,veng,all
outres,fflux,all
outres,cont,all

```

```

/nopr
esel,s,type,,137
cm,_elmisc,elem
esel,all
/gopr
outres,misc,all,_elmisc
cnvtol,heat,,.001,,1.e-006 ! Program Controlled. Set MINREF equivalent
    of 1e-6 Watts
! ***** Begin Command Snippet *****
*TOPER,inner_table_aux,inner_table,add,inner_table, 8.330000000000000e
    -07,0,0
BFE,inner_table_selection,HGEN,1,%inner_table_aux%

! ***** End Command Snippet *****
! ***** Begin Command Snippet *****
*TOPER,outer_table_aux,outer_table,add,outer_table, 8.330000000000000e
    -07,0,0
BFE,outer_table_selection,HGEN,1,%outer_table_aux%

! ***** End Command Snippet *****
! ***** WB SOLVE COMMAND *****
! check interactive state
*get,ANSINTER_,active,,int
*if,ANSINTER_,ne,0,then
/eof
*endif
solve
/com ***** Write FE CONNECTORS *****
CEWRITE,file,ce,,INTE
/com,*****
/com,***** FINISHED SOLVE FOR LS 1 *****
/com,*****

/com,***** SOLVE FOR LS 2 OF 9 *****
/nopr
/gopr
autots,off ! User turned off automatic time stepping
nsub,10,10,10
time,1.25e-006
timint,on ! Turn on time integration effects
outres,erase
outres,all,none
outres,nsol,all
outres,rsol,all
outres,eangl,all
outres,veng,all
outres,fflux,all
outres,cont,all
outres,misc,all,_elmisc

```

```

cnvtol,heat,,.001,,1.e-006 ! Program Controlled. Set MINREF equivalent
of 1e-6 Watts
! ***** Begin Command Snippet *****
*TOPER,inner_table_aux,inner_table,add,inner_table, 1.000000000000000e
+00,0,0
BFE,inner_table_selection,HGEN,1,%inner_table_aux%

! ***** End Command Snippet *****
! ***** Begin Command Snippet *****
*TOPER,outer_table_aux,outer_table,add,outer_table, 1.000000000000000e
+00,0,0
BFE,outer_table_selection,HGEN,1,%outer_table_aux%

! ***** End Command Snippet *****
solve
/com,*****
/com,***** FINISHED SOLVE FOR LS 2 *****
/com,*****
/com,***** SOLVE FOR LS 3 OF 9 *****
/nopr
/gopr
autots,off ! User turned off automatic time stepping
nsub,10,10,10
time,1.552e-006
timint,on ! Turn on time integration effects
outres,erase
outres,all,none
outres,nsol,all
outres,rsol,all
outres,eangl,all
outres,veng,all
outres,fflux,all
outres,cont,all
outres,misc,all,_elmisc
cnvtol,heat,,.001,,1.e-006 ! Program Controlled. Set MINREF equivalent
of 1e-6 Watts
! ***** Begin Command Snippet *****
BFEDELE,inner_table_selection,ALL

! ***** End Command Snippet *****
! ***** Begin Command Snippet *****
BFEDELE,outer_table_selection,ALL

! ***** End Command Snippet *****
solve
/com,*****
/com,***** FINISHED SOLVE FOR LS 3 *****
/com,*****
/com,***** SOLVE FOR LS 4 OF 9 *****
/nopr

```

```

/gopr
autots,off                ! User turned off automatic time stepping
nsub,10,10,10
time,1.802e-006
timint,on                ! Turn on time integration effects
outres,erase
outres,all,none
outres,nsol,all
outres,rsol,all
outres,eangl,all
outres,veng,all
outres,fflux,all
outres,cont,all
outres,misc,all,_elmisc
cnvtol,heat,,.001,,1.e-006 ! Program Controlled. Set MINREF equivalent
    of 1e-6 Watts
! ***** Begin Command Snippet *****
*TOPER,inner_table_aux,inner_table,add,inner_table, 1.000000000000000e
    +00,0,0
BFE,inner_table_selection,HGEN,1,%inner_table_aux%

! ***** End Command Snippet *****
! ***** Begin Command Snippet *****
*TOPER,outer_table_aux,outer_table,add,outer_table, 1.000000000000000e
    +00,0,0
BFE,outer_table_selection,HGEN,1,%outer_table_aux%

! ***** End Command Snippet *****
solve
/com,*****
/com,***** FINISHED SOLVE FOR LS 4 *****
/com,*****
/com,***** SOLVE FOR LS 5 OF 9 *****
/nopr
/gopr
autots,off                ! User turned off automatic time stepping
nsub,10,10,10
time,2.104e-006
timint,on                ! Turn on time integration effects
outres,erase
outres,all,none
outres,nsol,all
outres,rsol,all
outres,eangl,all
outres,veng,all
outres,fflux,all
outres,cont,all
outres,misc,all,_elmisc
cnvtol,heat,,.001,,1.e-006 ! Program Controlled. Set MINREF equivalent
    of 1e-6 Watts

```



```

! ***** Begin Command Snippet *****
BFEDELE,inner_table_selection,ALL

! ***** End Command Snippet *****
! ***** Begin Command Snippet *****
BFEDELE,outer_table_selection,ALL

! ***** End Command Snippet *****
solve
/com,*****
/com,***** FINISHED SOLVE FOR LS 5 *****
/com,*****
/com,***** SOLVE FOR LS 6 OF 9 *****
/nopr
/gopr
autots,off          ! User turned off automatic time stepping
nsub,10,10,10
time,2.354e-006
timint,on           ! Turn on time integration effects
outres,erase
outres,all,none
outres,nsol,all
outres,rsol,all
outres,eangl,all
outres,veng,all
outres,fflux,all
outres,cont,all
outres,misc,all,_elmisc
cnvtol,heat,,.001,,1.e-006 ! Program Controlled. Set MINREF equivalent
    of 1e-6 Watts
! ***** Begin Command Snippet *****
*TOPER,inner_table_aux,inner_table,add,inner_table, 1.000000000000000e
    +00,0,0
BFE,inner_table_selection,HGEN,1,%inner_table_aux%

! ***** End Command Snippet *****
! ***** Begin Command Snippet *****
*TOPER,outer_table_aux,outer_table,add,outer_table, 1.000000000000000e
    +00,0,0
BFE,outer_table_selection,HGEN,1,%outer_table_aux%

! ***** End Command Snippet *****
solve
/com,*****
/com,***** FINISHED SOLVE FOR LS 6 *****
/com,*****
/com,***** SOLVE FOR LS 7 OF 9 *****
/nopr
/gopr
autots,off          ! User turned off automatic time stepping

```

```

nsub,10,10,10
time,2.656e-006
timint,on                ! Turn on time integration effects
outres,erase
outres,all,none
outres,nsol,all
outres,rsol,all
outres,eangl,all
outres,veng,all
outres,fflux,all
outres,cont,all
outres,misc,all,_elmisc
cnvtol,heat,,.001,,1.e-006 ! Program Controlled. Set MINREF equivalent
    of 1e-6 Watts
! ***** Begin Command Snippet *****
BFEDELE,inner_table_selection,ALL

! ***** End Command Snippet *****
! ***** Begin Command Snippet *****
BFEDELE,outer_table_selection,ALL

! ***** End Command Snippet *****
solve
/com,*****
/com,***** FINISHED SOLVE FOR LS 7 *****
/com,*****
/com,***** SOLVE FOR LS 8 OF 9 *****
/nopr
/gopr
autots,off                ! User turned off automatic time stepping
nsub,10,10,10
time,2.906e-006
timint,on                ! Turn on time integration effects
outres,erase
outres,all,none
outres,nsol,all
outres,rsol,all
outres,eangl,all
outres,veng,all
outres,fflux,all
outres,cont,all
outres,misc,all,_elmisc
cnvtol,heat,,.001,,1.e-006 ! Program Controlled. Set MINREF equivalent
    of 1e-6 Watts
! ***** Begin Command Snippet *****
*TOPER,inner_table_aux,inner_table,add,inner_table, 1.000000000000000e
    +00,0,0
BFE,inner_table_selection,HGEN,1,%inner_table_aux%

! ***** End Command Snippet *****

```

```

! ***** Begin Command Snippet *****
*TOPER,outer_table_aux,outer_table,add,outer_table, 1.000000000000000e
+00,0,0
BFE,outer_table_selection,HGEN,1,%outer_table_aux%

! ***** End Command Snippet *****
solve
/com,*****
/com,***** FINISHED SOLVE FOR LS 8 *****
/com,*****
/com,***** SOLVE FOR LS 9 OF 9 *****
/nopr
/gopr
autots,on                ! User turned on automatic time stepping
nsub,72,96,60,OFF
time,2.e-004
timint,on                ! Turn on time integration effects
outres,erase
outres,all,none
outres,nsol,all
outres,rsol,all
outres,eangl,all
outres,veng,all
outres,fflux,all
outres,cont,all
outres,misc,all,_elmisc
cnvtol,heat,,.001,,1.e-006 ! Program Controlled. Set MINREF equivalent
of 1e-6 Watts
! ***** Begin Command Snippet *****
BFEDELE,inner_table_selection,ALL

! ***** End Command Snippet *****
! ***** Begin Command Snippet *****
BFEDELE,outer_table_selection,ALL

! ***** End Command Snippet *****
solve
/com,*****
/com,***** FINISHED SOLVE FOR LS 9 *****
*get,_wallasol,active,,time,wall
/post1
xmlo,ENCODING,ISO-8859-1
xmlo,parm
/xml,parm,xml
fini
/gopr
*get,_walldone,active,,time,wall
_preptime=(_wallbsol-_wallstrt)*3600
_solvertime=(_wallasol-_wallbsol)*3600
_posttime=(_walldone-_wallasol)*3600

```

```
_totaltim=(_walldone-_wallstrt)*3600
*get,_dlbratio,active,0,solu,dlbr
*get,_comptime,active,0,solu,comb
*get,_ssmode,active,0,solu,ssmm
*get,_ndofs,active,0,solu,ndof
/fclean      !clean distributed files
/com,--- Total number of nodes = %_nummode%
/com,--- Total number of elements = %_numelem%
/com,--- Element load balance ratio = %_dlbratio%
/com,--- Time to combine distributed files = %_comptime%
/com,--- Sparse memory mode = %_ssmode%
/com,--- Number of DOF = %_ndofs%
/wb,file,end      ! done with WB generated input
```

List of Figures

1.1	The CERN accelerator complex	2
1.2	General view of the ISOLDE area. The incoming proton beam line and the bifurcation between GPS and HRS lines is visible, as well as the dumps and the experimental area	4
1.3	View of the GPS target station. The incoming proton beam hits the target, and a percentage of the particles continues straight towards the beam dump. The other fraction of the beam is extracted and steered towards the Experimental Area by a combination of electric and magnetic fields	5
2.1	On the top, heading and first few lines of the output of a FLUKA simulation. On the bottom, a graphical representation of the cylindrical coordinate system and the resulting geometry division. The inner cylinder is not represented as it was contained in a separate text file with a finer geometry division	8
2.2	Time structure of the pulses which have been simulated. Each pulse consists of four bunches, with gaps in between them. Typically there would be a gap between pulses of either 1.2 or 2.4 seconds	9
2.3	Workflow example in ANSYS® Workbench. The results of a transient thermal simulation are imported into a transient structural simulation	10
3.1	Layout of the beam dump downstream of the GPS target position.	11
3.2	Layout of the beam dump downstream of the HRS target position.	12
3.3	Section showing the HRS dump in red, the concrete blocks in grey, and the soil in green.	12
3.4	On the top, the HRS dump blocks. On the bottom, the GPS dump blocks. The concrete blocks are not shown. The red arrow shows the direction of the beam. The dimensions shown are in meters	13
3.5	ISOLDE target: the upper, longer cylinder is the target container, while the shorter cylinder is the neutron converter	13
3.6	Picture of the HRS Faraday cage with the cover for MEDICIS target irradiations.	14
3.7	Thermocouple (center) with two magnets at each side. The thermocouple itself also includes magnets above and below.	15
3.8	GPS dump face with both thermocouples installed.	16
3.9	HRS dump face with both thermocouples installed.	16
3.10	Installation of the thermocouples. The long arm used to insert the thermocouple is visible on the photo.	17
3.11	Intensity recorded during the GPS test.	17
3.12	Beam size recorded during the GPS test.	18
3.13	Intensity recorded during the HRS test.	18

3.14	Beam size recorded during the HRS test.	19
3.15	GPS setup	20
3.16	HRS setup. 2 planes of symmetry were used.	20
3.17	Graph showing the temperature evolution measured by the thermocouples vs the temperature simulated by the finite element simulation in the GPS dump.	22
3.18	Graph showing the temperature evolution measured by the thermocouples vs the temperature simulated by the finite element simulation in the HRS dump.	22
4.1	PSB dump. On the left the size and shape of the dump is shown, with dimensions in mm. On the right, a schematic shows how the dump was air-cooled	27
4.2	Preliminary model of the water-cooled, tantalum-cladded tungsten dump. In the image, the beam would come from the right	27
4.3	Half view of the air-cooled dump, including the outer enclosure with the inlet and outlet pipes, and the dump block with its cooling fins	29
4.4	Quarter view of downstream section of a shorter actively cooled dump, showing the steady-state temperatures	30
4.5	Quarter view of the new dump design	31
4.6	Von Mises stress results in the shrink-fitting FE model	32
4.7	Temperature evolution on the graphite (left) and the CuCr1Zr (right) over the first 4 ms. The effect of the 4 particle bunches is clearly visible	33
4.8	Christensen criterion for the graphite, with a maximum of 0.27	33
4.9	Von Mises stress in the CuCr1Zr, with a maximum of 53 MPa that is however heavily influenced by the local contact boundary conditions	34
4.10	Von Mises stress in the center of the upstream face of the CuCr1Zr, with a maximum of 21 MPa	34
4.11	Schematic of the division for the dump manufacturing: first the three CuCr1Zr parts and the cooling pipes would go through the HIP process, and then the graphite diluter would be inserted	35
4.12	Temperature results (shown in Kelvin) of the simulation of the power deposition on the surrounding shielding	36
4.13	Temperature evolution on the graphite (left) and the CuCr1Zr (right) over the first 4 ms with a target installed	37

List of Tables

3.1	Current and future operating parameters.	14
3.2	Data for the target that was used in the simulations in this chapter.	15
3.3	Parameters used in both simulations.	21
3.4	Results for different energies and intensities. See section 3.7 for more information	24
4.1	Beam parameters for future dump design.	26
4.2	Results of the early designs. The quoted maximum temperatures and stresses are for the CuCr1Zr. During the early designs the beam parameters were slightly different to the ones that were finally chosen	27
4.3	Cooling parameters comparison	28
4.4	Air-cooling results	29
4.5	Water-cooling results	29
4.6	Material properties for the future dump design	31
4.7	Final values for HTC calculation using the Dittus-Boelter equation	32
4.8	Thermo-mechanical results for the future dump design	33
4.9	Thermal results of the proposed dump with a target installed	36
4.10	Thermo-mechanical results for the future dump design using the design scenario of 5 consecutive shots with the smallest (accident) beam size.	37

Bibliography

- [1] “CERN - our history,” 2024. Available at <https://home.cern/about/who-we-are/our-history>.
- [2] “CERN - our member states,” 2024. Available at <https://home.cern/about/who-we-are/our-governance/member-states>.
- [3] “LHC - the guide,” 2021. Available at <https://cds.cern.ch/record/2809109/files/CERN-Brochure-2021-004-Eng.pdf>.
- [4] R. Catherall *et al.*, “The ISOLDE facility,” *Journal of Physics G: Nuclear and Particle Physics*, vol. 44, no. 094002, 2017.
- [5] Ansys[®], “Ansys Mechanical Enterprise.”
- [6] T. Böhlen, F. Cerutti, M. Chin, A. Fassò, A. Ferrari, P. G. Ortega, A. Mairani, P. R. Sala, G. Smirnov, and V. Vlachoudis, “The FLUKA code: developments and challenges for high energy and medical applications,” *Nuclear data sheets*, vol. 120, pp. 211–214, 2014.
- [7] R. M. Christensen, “A comprehensive theory of yielding and failure for isotropic materials,” 2007.
- [8] B. Conde Fernandez *et al.*, “Safety File for CERN-MEDICIS, Descriptive Part,” tech. rep., CERN, Geneva, 2019. Available at <https://edms.cern.ch/document/1541088>.
- [9] B. Jonson *et al.*, “ISOLDE PS Booster facility at CERN; experiments with slow radioactive beams,” *Nuclear Physics News*, vol. 3, no. 2, 1993.
- [10] V. Venturi, “ISOLDE dumps: evaluation of present and future operation,” tech. rep., CERN, Geneva, 2013. Available at <https://edms.cern.ch/document/1277863>.
- [11] G. drawing, “ISOLDE 2EME ETAPE BEAM DUMP GPS,” tech. rep., CERN, Geneva, 2006. Available at <https://edms.cern.ch/document/129078>.
- [12] H. drawing, “ISOLDE 2EME ETAPE BEAM DUMP HRS,” tech. rep., CERN, Geneva, 2006. Available at <https://edms.cern.ch/document/129308>.
- [13] C. Lamberet, “Bilan du Matériel radioactive utilise comme blindage dans le complexe ISOLDE,” tech. rep., CERN, Geneva, 1992. Available at <https://edms.cern.ch/document/2250353>.
- [14] S. Kalogirou and G. Florides, “Measurements of ground temperature at various depths,” 01 2004.

- [15] MeteoSwiss, “Air temperature at Genève / Cointrin,” May 2023.
- [16] C. Madhusudana, *Thermal contact conductance*. Springer International Publishing, 2014.
- [17] J. R. Davis, *Cast Irons*. ASM Specialty Handbook, 1996.
- [18] *ASM Handbook, Volume 1: Properties and Selection: Irons, Steels, and High-Performance Alloys*. ASM Handbook Committee, 1990.
- [19] M. Fraser *et al.*, “Functional Specification for the ISOLDE Beam Dump Upgrade,” tech. rep., CERN, Geneva, 2023. Available at <https://edms.cern.ch/document/2891725>.
- [20] A. Perillo-Marcone *et al.*, “Design and operation of the air-cooled beam dump for the extraction line of CERN’s proton synchrotron booster,” *Physical review accelerators and beams*, vol. 23, no. 063001, 2020.
- [21] Kupferdatenblatt, “CuCr1Zr technical report,” 2005. Available at <https://kupfer.de/wp-content/uploads/2019/11/CuCr1Zr.pdf>.
- [22] M. Kawai, K. Kikuchi, K. H., J.-F. Li, and M. Furusaka, “Fabrication of a tantalum-clad tungsten target for kens,” *Journal of nuclear materials*, vol. 296, no. 1-3, pp. 312–320, 2001.
- [23] R. Lillard, D. Pile, and D. Butt, “The corrosion of materials in water irradiated by 800 mev protons,” *Journal of nuclear materials*, vol. 278, no. 2-3, pp. 277–289, 2000.
- [24] H. V. Atkinson and S. Davies, “Fundamental aspects of hot isostatic pressing: An overview,” *Metallurgical and Materials Transactions A*, vol. 31, pp. 2981–3000, 2000.
- [25] A. Yegyan Kumar, Y. Bai, A. Eklund, and C. B. Williams, “The effects of hot isostatic pressing on parts fabricated by binder jetting additive manufacturing,” *Additive Manufacturing*, vol. 24, pp. 115–124, 2018.
- [26] J. Wu, R. Guo, L. Xu, Z. Lu, Y. Cui, and R. Yang, “Effect of hot isostatic pressing loading route on microstructure and mechanical properties of powder metallurgy Ti2AlNb alloys,” *Journal of Materials Science Technology*, vol. 33, no. 2, pp. 172–178, 2017.
- [27] S. Pianese *et al.*, “Hot isostatic pressing assisted diffusion bonding for application to the super proton synchrotron internal beam dump at CERN,” *Physical review accelerators and beams*, vol. 24, no. 043001, 2021.
- [28] SGL carbon, “Datasheet.” Available at <https://www.sglcarbon.com/data/pdf/SGL-Datasheet-SIGRAFINE-R4550-EN.pdf>.
- [29] F. Incropera and D. DeWitt, *Fundamentals of Heat and Mass Transfer*. John Wiley & Sons, 1996.